J 20 419 F

A Publication
for the Radio-Amateur
Especially Covering VHF,
UHF and Microwaves

VHF communications

Volume No. 16 · Spring · 1/1984 · DM 6.50

10 GHz Transceiver with Dielectrically Stabilised Oscillator

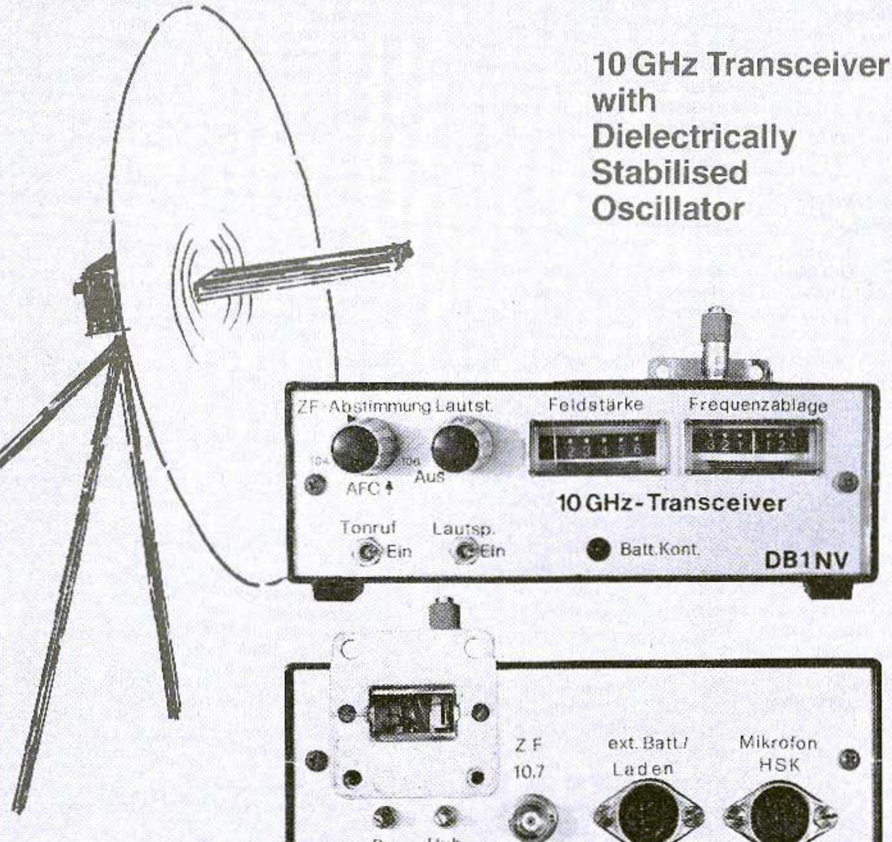

VHF communications

A Publication for the Radio Amateur
Especially Covering VHF, UHF, and Microwaves

Volume No. 16 · Spring · Edition 1/1984

Published by: Verlag UKW-BERICHTE, Terry Bittan, Jahnstrasse 14, D-8523 BAIERSDORF, Fed. Rep. of Germany, Telephones (91 33) 855, 856.

Publisher: Terry Bittan, DJ 0 BQ

Editors: Terry D. Bittan, G 3 JVQ / DJ 0 BQ, responsible for the text
Robert E. Lentz, DL 3 WR, responsible for the technical contents

Advertising manager: Terry Bittan

VHF COMMUNICATIONS The international edition of the German publication UKW-BERICHTE, is a quarterly amateur radio magazine especially catering for the VHF/UHF/SHF technology. It is published in Spring, Summer, Autumn, and Winter. The 1983 subscription price is DM 22.00 or national equivalent per year. Individual copies are available at DM 6,50 or equivalent, each. Subscriptions, orders of individual copies, purchase of PC-boards and advertised special components, advertisements and contributions to the magazine should be addressed to the national representative.

Printed in the Fed. Rep. of Germany by R. Reichenbach KG. Krelingstr. 39 · 8500 Nuernberg.

We would be grateful if you would address your orders and queries to your representative.

Representatives

Austria
Verlag UKW-BERICHTE, Terry D. Bittan
POB 80, D-8523 Baiersdorf/W. Germany
Creditanstalt Bankverein, WIEN Kto. 17-90.599,
PSchKto WIEN 1.169.146

Australia
WIA PO Box 150, TOORAK, VIC 3142, Tel.24-8652

Belgium
COMELEC, D. Wilmus, Rue de Juifs, 26,
7000 MONS, Tel. 065/31 60 97
Stereohouse, Brusselsesteenweg 416, B-9218 GENT,
PCR 000-1014257 CCP, Tel. (091) 31 21 11

Denmark
Halskov Electronic, OZ 7 LX, Sigersted gamle Skole,
DK-4100 Ringsted, Telf. 03-616162, Giro 7 29 68 00.

France
Christiane Michél, F 5 SM, SM Electronic,
20 bis, Avenue des Clairions, F-89000 AUXERRE
Tel. (86) 46 96 59

Finland
Erkki Hohenthal, SF-31400 SOMERO
Joensuuntie 6, Tel. 924-46311

Holland
MECOM, PA 0 AER, PO Box 40, Coendersstraat 24,
NL-9780 AA BEDUM, Tel.05900-14390,
Postgiro 3986163

Israel
Z. Pomer, 4X4KT, PO Box 222, K. MOZKIN 26114
Tel. 00972-4714078

Italy
Franco Armenghi, I 4 LCK, Via Sigonio 2,
I-40137 BOLOGNA, Tel. (051) 34 56 97

Luxembourg
TELECO, Jos. Faber, LX 1 DE, 5-9, Rue de la fontaine,
ESCH-SUR-ALZETTE, Tel. 53752

New Zealand
E. M. Zimmermann, ZL 1 AGQ, PO Box 31-261
Milford, AUCKLAND 9, Phone 492-744

Norway
Henning Theg, LA 4 YG, Postboks 70,
N-1324 LYSAKER, Postgirokonto 3 16 00 09

South Africa
SA Publications, PO Box 2232, JOHANNES-
BURG 2000, Telephone 22-1496

Spain + Portugal
Julio A. Prieto Alonso, EA 4 CJ, MADRID-15,
Donoso Cortés 58 5°-B, Tel. 243 83 84

Sweden
Sven Hubermark, SM 5 DDX, Postbox 2090,
S-14102 HUDDINGE

Switzerland
Terry Bittan, Schweiz.Kreditanstalt ZÜRICH,
Kto.469.253-41; PSchKto.ZÜRICH 80-54.849

USA
Data Service Co., KØRC
3110 Evelyn Street, ROSEVILLE MI 55113, Tel. (612) 636-9469

Contents

UKWberichte Terry D. Bittan · Jahnstr. 14 · Postfach 80 · D-8523 Baiersdorf
Tel. West Germany 9133-855. For Representatives see cover page 2

Jochen Jirmann, DB 1 NV

A FM-Transceiver for 10 GHz with dielelectrically-stabilized Oscillator

The GaAs-FET doubler module FO-DP12, or FO-DP13 described in the previous edition of VHF COMMUNICATIONS (1) is especially suitable for construction of a small 10 GHz transceiver for wideband FM. The current drain of the dielectrically-stabilized oscillator is three to four times less than that of a Gunn oscillator with straight-through mixer; this is a great advantage for portable operation.

Table 1 gives the specifications of the transceiver:

Microwave module:	FO-DP12 or FO-DP13
Frequency range:	10.25–10.45 GHz
Operating mode:	Wideband FM, frequency shift 105 MHz or 30 MHz, according to IF
Transmit power:	4–5 mW
Noise figure:	Approx. 12–15 dB (comparable with a Gunnplexer)
Operating voltage:	12 V / 150 mA

The dimensions of the compact, author's prototype **(Figure 1)** are 150 × 120 × 55 mm; the total weight of 800 g also includes an accumulator with a capacity of 225 mAh, which is sufficient for one hour's operation, without external power sources.

The transceiver comprises the following modules: A modified doubler module FO-DP12KF, or FO-DP13KF, an IF/AF-module, the voltage stabilizer for the FET-oscillator, and a modulation amplifier complete with dot generator.

1. DOUBLER MODULE

As has already been described, the FET-oscillator tuned to 10.525 GHz is provided with one or two mixer diodes, which are used as straight-through mixer. For amateur applications, it is necessary for the frequency to be pulled into the amateur band and for the fixed tuning to be made variable. This is achieved by modifying the module as follows:

The cover complete with the tuning screw can be removed after carefully bending up the tabs. The ceramic laminate on which the microwave circuit is built up should not be touched! It is now possible for the tuning screw to be replaced by a miniature micrometer, or by a M5-screw with a fine thread together with a matching bushing.

Attention should be paid that no play is present; this is also valid when using a Gunn

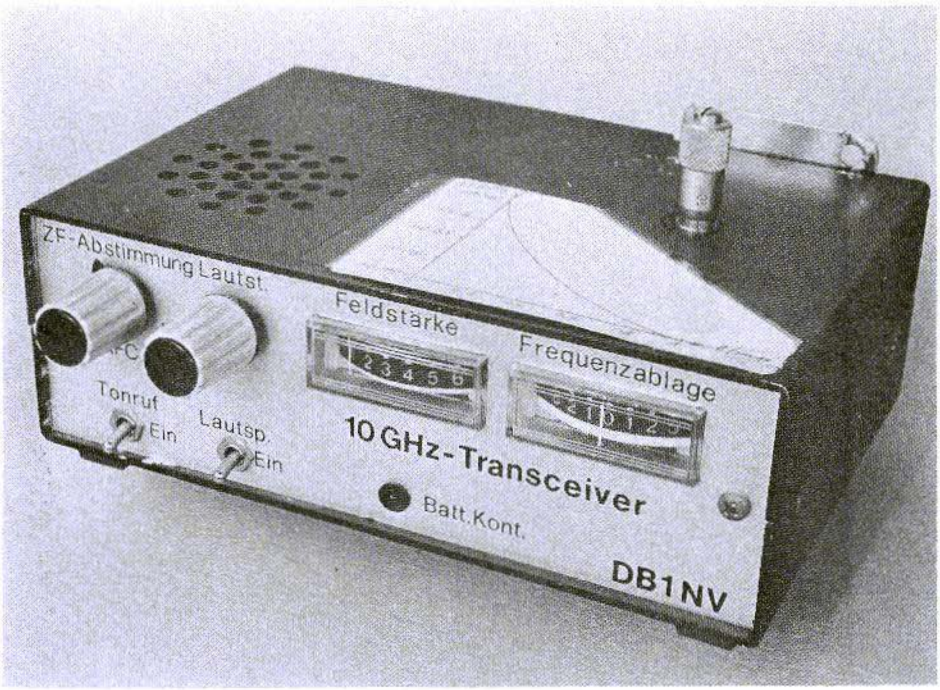

Fig. 1: The 10 GHz FM-transceiver described by the author

oscillator. The cover then is replaced and soldered around the edge with the aid of a large soldering iron **(Figure 2)**. The tuning can now be made with the aid of an absorption wavemeter **(Figure 3)**.

Finally, a tip: Since FETs and mixer diodes are very sensitive to static charge, it is important that all connections of the module are connected to the case until they are installed into place.

2. IF-AMPLIFIER

A large number of IF-circuits have been described for 10 GHz transceivers. These, however, have all required additional modules such as preamplifiers, squelches, AFC-modules, etc. The IF-circuit to be described does not require any external modules, only the external controls, and its dimensions are very compact (72 mm x 145 mm). The module can also be used as 144 MHz FM-receiver by changing a few components.

The IF-module is designed for a frequency of 105 MHz, but can also be modified for 30 MHz. However, in this case one must expect a 1 to 2 dB inferior system noise figure, since part of the noise sidebands of the microwave oscillator will be converted back to IF-level. Considering the large number of 30 MHz-systems operating in conjunction with Gunn oscillators, it is surprising that this is not common knowledge.

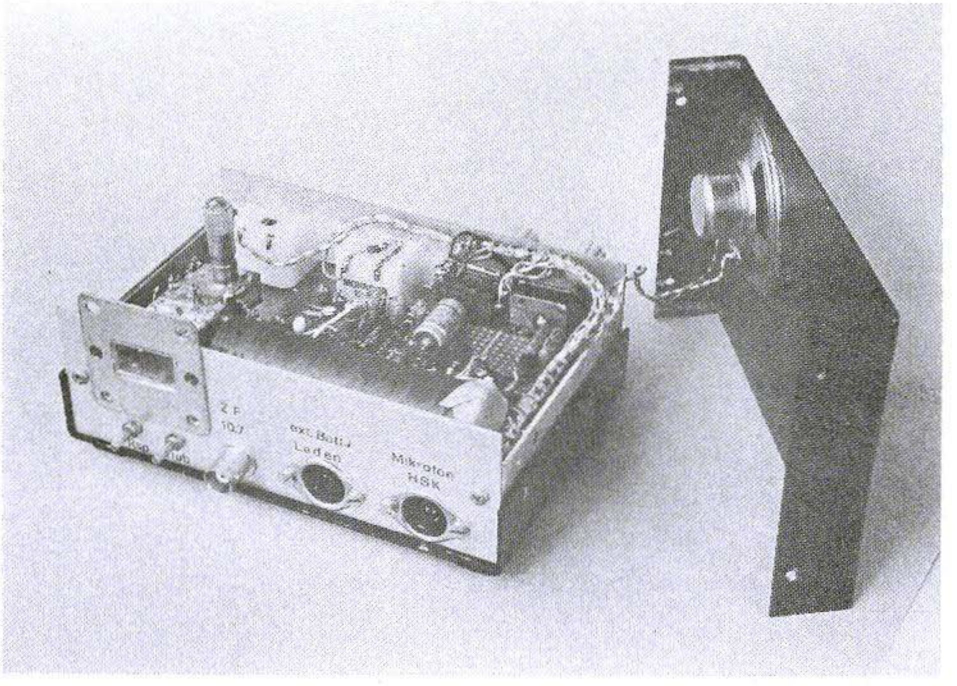

Fig. 2: Voltage stabilizer for the oscillator, as well as the modulator are built up on Vero boards in the author's prototype

2.1. Concept

The module operates at an intermediate frequency of 105 MHz, and can be tuned electronically by ±1 MHz. The input is designed for direct connection to a conventional mixer diode (IF-impedance approx. 300 Ω). The noise figure of the IF-circuit is better than 2 dB. In order to increase the sensitivity of the receiver further, the IF-bandwidth was reduced to 100 kHz, and a lowpass filter having a cutoff frequency of 3 kHz, and a slope of 18 dB/ octave was provided in the audio amplifier.

The automatic fine tuning operates at the intermediate frequency of 105 MHz. This solves all problems with respect to the control direction of the AFC, which is required when controlling the microwave oscillator.

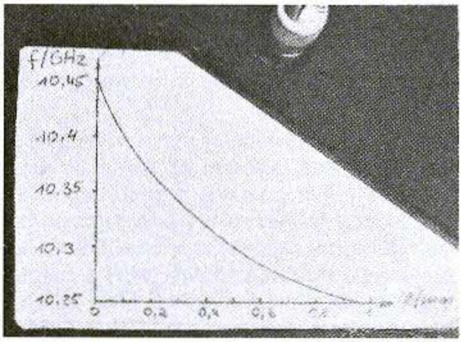

Fig. 3: The calibrated scale of the transceiver

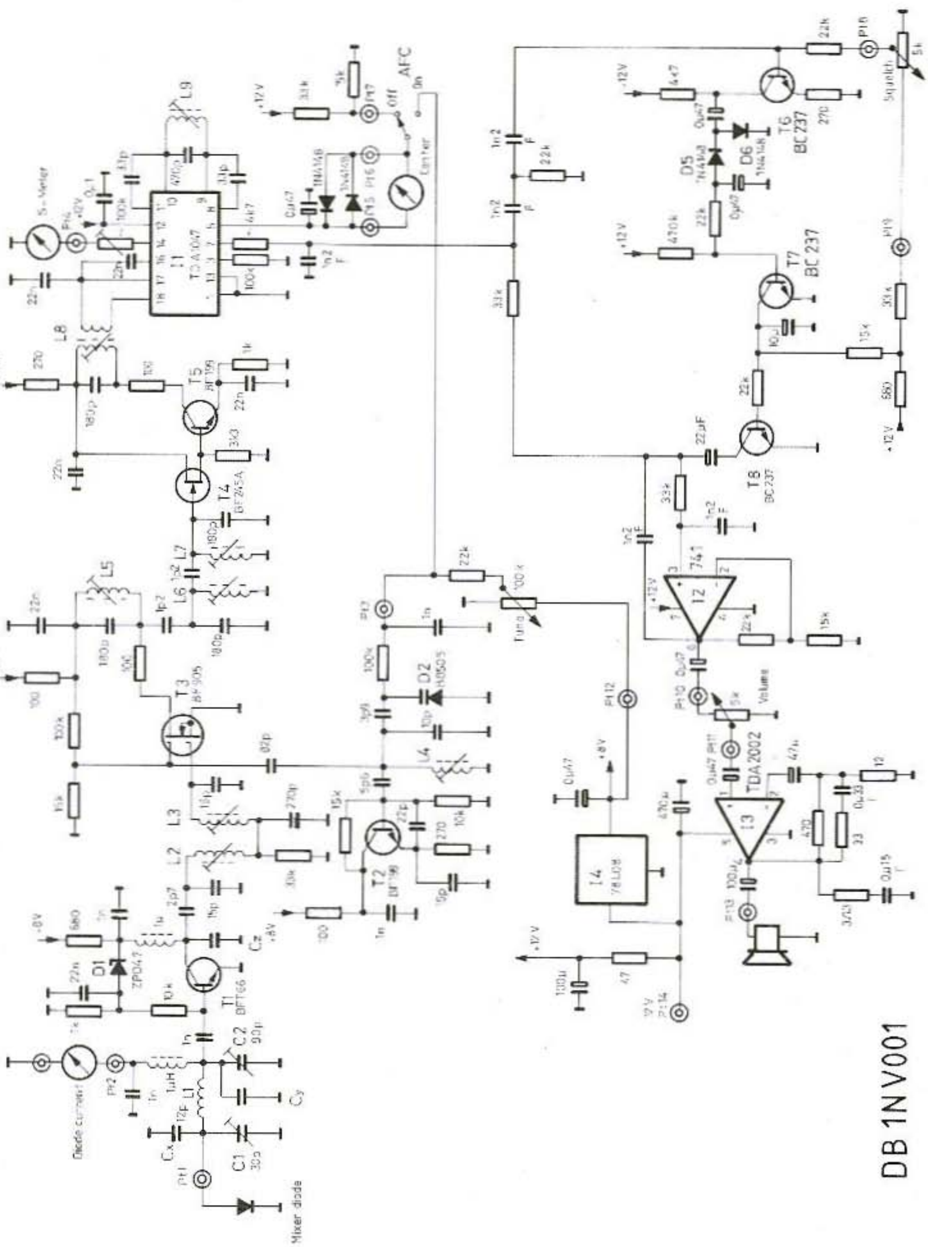

Fig. 4: Circuit diagram of the complete RF/IF/AF-circuits DB1NV 001

The tuning range of max. 1 MHz is sufficient if the microwave oscillators are relatively stable. The circuit possesses a squelch using the conventional 8 kHz method, and is provided with an efficient AF-amplifier **(Figure 4)**.

2.2. Circuit Description

The mixer diode of the microwave circuit is connected with the aid of a short piece of coaxial cable (max. 10 cm) to the input of the IF-amplifier. The variable network comprising L 1 and the two trimmers C 1 and C 2 transforms the impedance of the diode (approx. 300 Ω) to the input impedance of the preamplifier transistor T 1 (BFT 66). The real component of the input impedance is approximately 80 Ω. A meter for monitoring the diode current can be connected to Pt 2. If this is not required, Pt 2 should be grounded. The operating point of the BFT 66 is stabilized with the aid of a zener diode to $U_{CE} = 6$ V/$I_C = 3$ mA.

The preamplifier is followed by a two-stage bandpass filter. The bandwidth of the filter is in the order of 2 MHz, and the coupling is slightly overcritical. The subsequent mixer stage equipped with a dualgate MOSFET BF 905 converts the 105 MHz ±1 MHz-signal to the second intermediate frequency of 10.7 MHz. The local oscillator equipped with a BF 199, oscillates at 115.7 ±1 MHz and is tuned with the aid of a varactor diode BB 505. A voltage of 1 to 8 V at Pt 3 is necessary to cover the whole tuning range. VHF-preamplifier, mixer, and oscillator are operated from a stabilized voltage of 8 V from a 78 LO8. This voltage is available at pin 12 for further applications (e.g. transmit modulator).

The main selectivity of the IF-circuit is made in the LC-filter following the mixer. This three-stage filter is undercritically coupled, and possesses a bandwidth of approximately 100 kHz, which is the ideal bandwidth for a wide-band FM-signal having a frequency deviation of 40 to 50 kHz, and a maximum modulation frequency of 3 kHz. The PC-board is designed so that a 10.7 MHz crystal filter (such as QF 10.7–30) can be installed instead of L 6 and L 7. This allows the module to also be used for narrow-band FM-systems, and as a FM-receiver for 144 MHz.

The matching amplifier equipped with T 4 (BF 245) and T 5 (BF 199) amplifies the 10.7 MHz-level to a level over that of the wideband noise generated in the FM-demodulator. An integrated circuit TDA 1047 is used for FM-demodulation, generation of the control voltage and tuning voltage.

The internal squelch of this integrated circuit is designed for broadcast applications and will not open until the signal is in excess of S9 when receiving amateur transmissions. For this reason, it was switched off by grounding pin 13. The internal AFC-switching is also not used (pin 2 remains disconnected). The phase-shift circuit for the FM-demodulator is tuned with the aid of L 9. An S-meter with a dynamic range of 50 dB can be connected to Pt 4. The AFC-output of the TDA 1047, pin 5, is a push-pull current source, which can supply or accept a maximum of 150 μA. This allows the AFC-circuit to be connected in parallel with the normal tuning voltage. As long as no frequency shift is present, the AFC-output will "float" together with the tuning voltage. The maximum hold range of the AFC is determined by the impedance of the tuning voltage source. In the circuit used here, the AFC-current is fed via the center-zerometer (±50 μA) either to the tuning diode of the oscillator, or when the AFC is switched off, to a voltage divider that is provided to ensure the correct operating point for the center-zerometer. Since many 10 GHz-stations only possess one meter which is switchable to S-meter and center-zero indication, two antiphase diodes are connected between Pt 5 and Pt 6; these secure the AFC-current path when the center-zerometer is switched off.

The demodulated signal from pin 7 of the TDA 1047 is passed through a lowpass filter (cutoff frequency = 12 kHz) for suppression of any residual IF, and is fed via a 33 kΩ resistor to the active AF-filter, and via a highpass filter (cutoff frequency = 6 kHz) to the noise amplifier T 6, which is equipped with a BC 237. After rectification of the noise, the resulting voltage is fed via a switching transistor (T 7) which controls the AF-switch T 8 (BC 237). The coupling from the collector of the switching transistor to the squelch potentiometer generates the necessary hysteris for optimum switching characteristics.

The operational amplifier I 2 (LM 741), and the AF-power amplifier I 3 (TDA 2002) form a Butterworth-lowpass filter with a cutoff frequency of 3 kHz and a slope of 18 dB/octave with the aid of their associated components. Any loudspeaker of at least 2 Ω impedance can be connected to the output.

2.3. Measured Results

Operating voltage range:	10–16 V
Current drain:	approx. 80 mA
VHF-bandwidth:	2 MHz
IF-bandwidth:	approx. 100 kHz
Noise figure:	< 2 dB
AF-output:	max. 5 W

2.4. Components

T 1:	BFT 66 (Siemens) possibly BFT 97 (pay attention to case!)
T 2, T 5:	BF 199, BF 241
T 3:	BF 900, BF 905 (Texas Instr.)
T 4:	BF 245 A (Texas Instr., Siemens)
T 6 ... T 8:	BC 237, BC 413, BC 550, or similar
D 1:	ZPD 4, 7 or C4V7 or similar zener diode
D 2:	BB 105, BB 505
D 3 – D 6:	1 N 4148 or similar
I 1:	TDA 1047 (Siemens)
I 2:	741, DIP 8
I 3:	TDA 2002 (SGS, Telefunken)
I 4:	LM 78 L08 (National), possibly 7808
L 1:	4.5 turns of 1 mm dia. silver-plated copper wire wound on a 5 mm former, self-supporting
L 2 – L 4:	4.5 turns of 0.5 mm dia. enamelled copper wire in a special coil set, 10 x 10 x 15 mm; yellow core
L 5 – L 7:	20 turns of 0.25 mm dia. enamelled copper wire in a special coil set, 10 x 10 x 15 mm; yellow or blue core
L 8:	20 turns + 6 turns, otherwise as L 5
L 9:	9 turns, otherwise as L 5 RFC: 2 miniature chokes 1 μH
C 1:	30 pF plastic foil trimmer, 7.5 mm dia. (Philips, red)
C 2:	90 pF plastic foil trimmer, 10 mm dia. (Philips, red). Other capacitors: Ceramic capacitors, min. 5 mm spacing.
Exceptions:	5 plastic foil capacitors, 1.2 nF, spacing 7.5 mm 1 plastic foil capacitor of 0.15 μF and 0.33 μF resp., spacing 7.5 mm.

Other bypass capacitors (22 nF, and 0 μ1): Ceramic tubular or multilayer capacitors.

Small electrolytics: Tantalum, or aluminium. Loudspeaker coupling electrolytic and bypass electrolytic for the operating voltage: Aluminium electrolytics, for horizontal mounting, 16 V, spacing 22.5 or 30 mm.

All resistors for 10 mm spacing.

2.5 Construction and Alignment

The circuit is accommodated on a double-coated PC-board (see **Figure 5**) whose dimensions are 70 mm x 144 mm. The PC-board has been designated DB1NV001. It is designed to be accommodated in a metal box of 72 x 145 x 25 mm. The upper side of the PC-board is in the form of a ground surface, and those components holes that are not grounded should be drilled out in the conventional manner **(Fig. 6)**. Attention should be paid to the manufacturing tolerances of the FETs T 4 (BF 245) during construction. A voltage of approximately 0.7 to 1.5 V must be present at the emitter of the BF 199 (T 5), otherwise it will be necessary to try another FET.

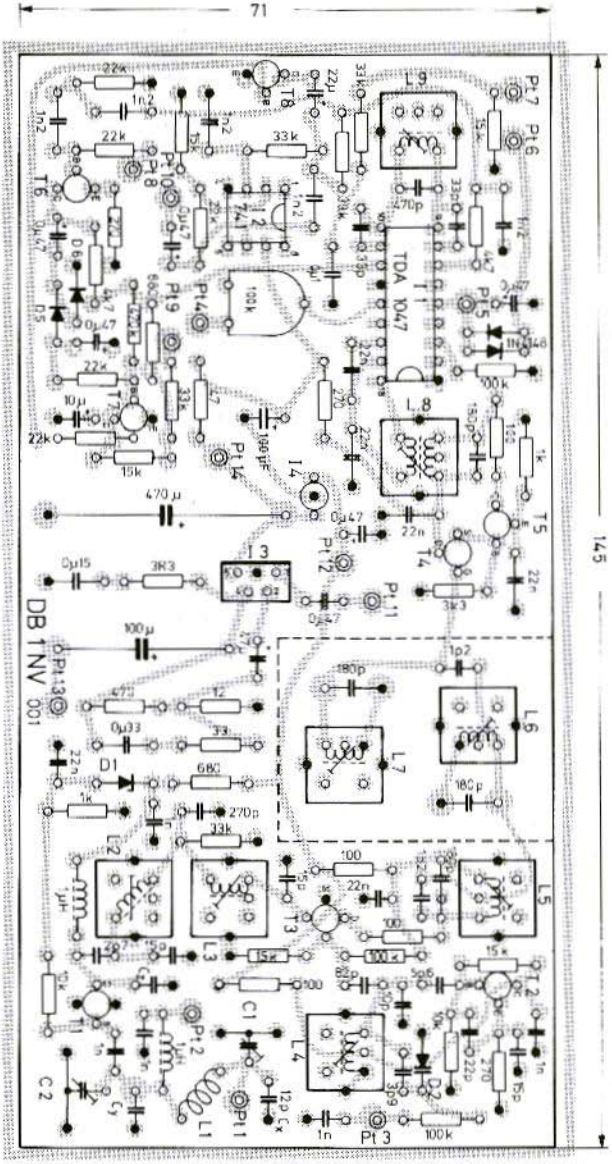

Fig. 5:
Component locations on the double-coated PC-board DB1NV 001

Point marked ● are to be soldered at both sides.

The integrated AF-amplifier is very advantageous due to its internal shortcircuit, overload, and over-temperature protection, as well as due to the low number of external components required; however, it possesses large manufacturing tolerances with respect to its quiescent current. One should select one having the lowest current drain. If the AF-amplifier oscillates, try and change the Boucherot-link (3.3 Ω/0.15 μF). The TDA 2002 need not be provided with a heat sink for normal output power levels.

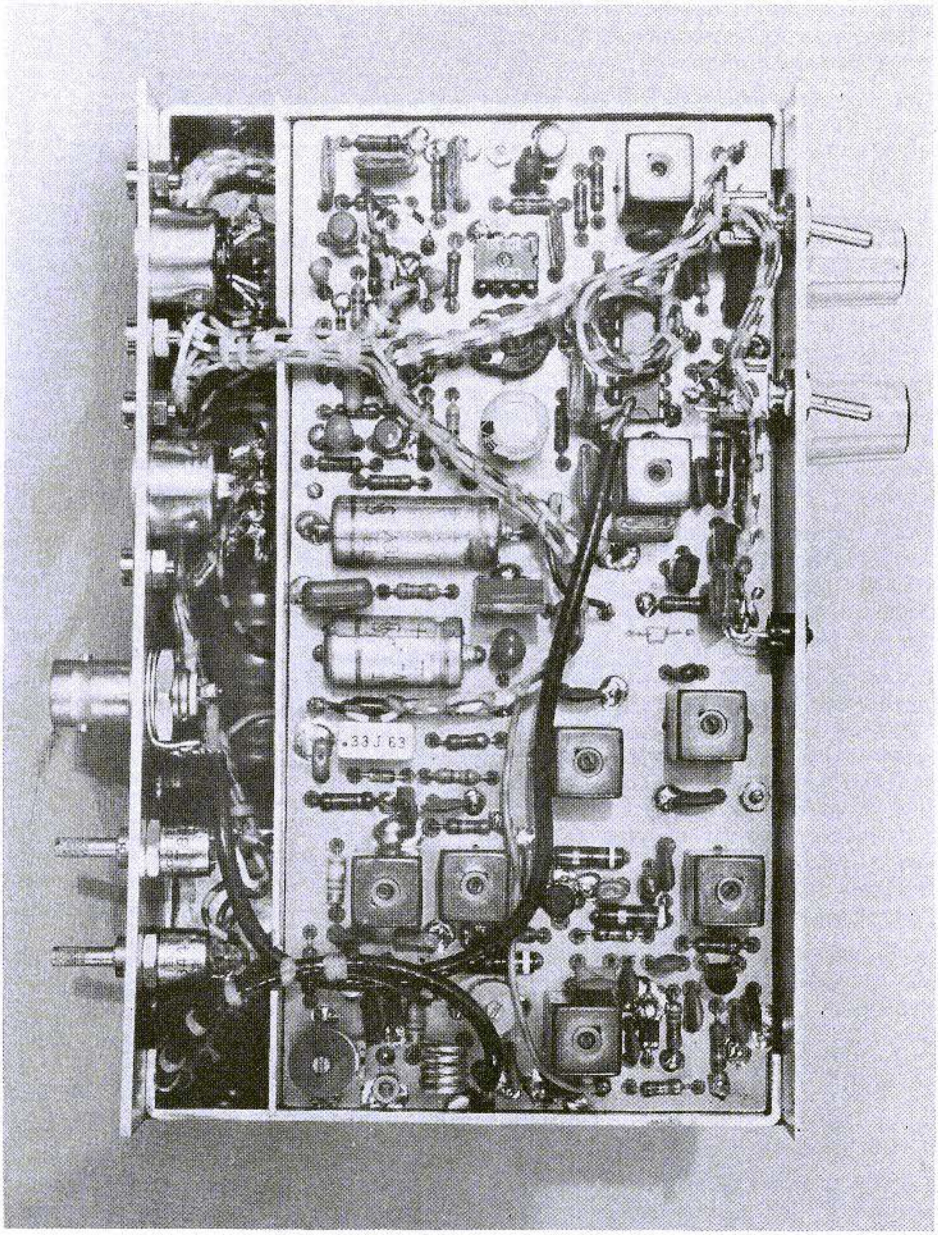

Fig. 6:
Photograph of the completed module DB1NV 001

The following are required for alignment: Multimeter, frequency meter, and a signal source for 105 MHz and 10.7 MHz.

Firstly check the voltage, directly after switching on, at Pt 12 (+8 V), as well as at the emitter of T 5 (+0.7 to 1.5 V), and at the collector of T 1 (+ 6 V).

Pt 4 is now connected to a suitable S-meter (e.g. 100 μA full scale), and a 10.7 MHz signal is fed to the gate of T 4. Inductances L 8 and L 9 are now aligned for maximum S-meter reading (the demodulator circuit including L 9 has a great effect on the S-meter).

The 10.7 MHz-signal is now fed to gate 1 of T 3; align L 5, L 6, and L 7 for maximum reading. A center-zero meter can now be connected between point 5 and 7, and inductance L 9 is aligned for zero.

This is followed by aligning the oscillator with the aid of L 4 to a center frequency of 115.7 MHz. The tuning range should amount to approximately 2 MHz when varying the voltage at Pt 3 from 1 V to 8 V.

The output of the 105 MHz signal source is now connected to the input via a resistor of 270 Ω. The signal generator should be terminated with 68 Ω. Align L 2, L 3, C 1, and C 2 for maximum S-meter reading. The trimmers C 1 and C 2 should be aligned later for best signal-to-noise ratio of the 10 GHz signal. If a swept-frequency generator is available, it is possible to subsequently align the filter comprising L 2/ L 3 to obtain a balanced passband curve.

No alignments are required in conjunction with the audio circuit, and it should operate immediately. The completed board is shown in **Figure 7**.

2.6 Modifications

If module DB1NV001 is to be used in conjunction with a lower input frequency than 105 MHz, the capacitance range of trimmers C 1 and C 2 of the input filter will not be large enough. For this reason, space has been provided for connecting two parallel capacitors,

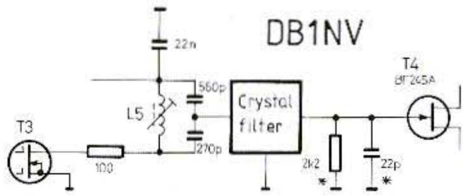

Fig. 7:
Circuit modification when using a crystal filter in the 10.7 MHz IF. The two components marked with * are mounted on the lower side of the board.

which are designated C_x and C_y in the component location plan.

If a tendency to oscillation is noticed in the input stage, it is possible for a capacitor (C_z in the component location plan) to be connected from the collector of T 1 to ground. The required value (a few pF) should be found experimentally.

It is also possible for the IF-filter comprising L 6 and L 7 to be replaced by a crystal filter such as the QF 10.7–30, when the module is to be used as a narrow-band FM-receiver. Some slight modifications must be made to the circuit:

The drain circuit of the mixer (L 5) transforms the output impedance of the DG-FET to the input impedance of the crystal filter of approx. 2.2 kΩ. The output of the crystal filter is also terminated with 2.2 kΩ/30 pF. If the passband curve can be swept, a 30 pF trimmer should be used instead of the fixed 22 pF capacitor, and aligned for minimum ripple in the passband range. **Figure 8** shows the required modifications when using a crystal filter.

When using the previously mentioned 30 kHz crystal filter in the IF, it is possible for module DB1NV001 to be used as miniature receiver for 145 MHz, if the input circuits are modified to this frequency. If the audio output is to be increased when receiving narrowband FM, the demodulator circuit of the TDA 1047/L 9 can be modified as described in (2).

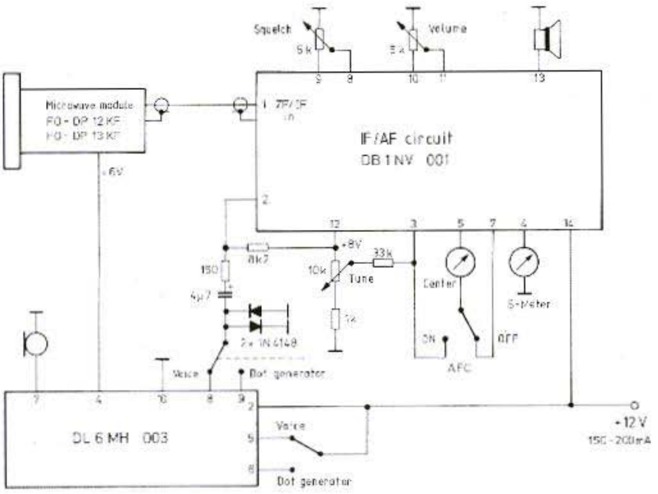

Fig. 8: Block diagram of the complete 10 GHz transceiver.

3. OTHER MODULES REQUIRED FOR TRANSCEIVE OPERATION

3.1. Voltage Stabilizer for the Oscillator

The FET-oscillator does not place any great demands on the supply voltage source. Any control circuit can be used that can supply 6 V at 50 mA. The simplest method is to use a fixed voltage stabilizer 7806, or 78L06.

3.2. Modulator

No reproducible results are obtained when modulating the frequency with the aid of the operating voltage, as is often the case with Gunn oscillators. Furthermore, the AM-component is very high. A far better solution is to modulate the externally impressed bias current for the mixer diode (0.5–1 mA); in this manner, it is possible to obtain a maximum frequency deviation of 200 kHz with a negligible AM-component. Any audio amplifier can be used as modulator, that can provide a voltage of 1 V_{pp} into 200 Ω. The author used a simple, two-stage audio amplifier with diode clipper, and a CMOS-oscillator as keyed sinewave oscillator (dot generator).

It is also possible to use module DL6MH 003. The voltage stabilizer provided on this board can be adjusted to 6 V, and will provide the supply voltage for the FET. A capacitor of 0.22 µF should be connected from pin 1 and pin 3 of the 7805 to ground in order to suppress any tendency to oscillation of this integrated voltage stabilizer.

4. INTERCONNECTION OF THE MODULES

The individual modules are interconnected as shown in **Figure 9**. Attention should be paid to the following: The IF-cable from the microwave module to the IF-amplifier should be kept as short as possible (max. 5 cm), otherwise, it will not be possible to match it to the mixer diode. When using module FO-DP12 KF, one selects the diode that provides the highest IF-level, and the other diode is left open-circuit. If voltage peaks appear at the output of the AF-amplifier on switching on and off, it is necessary to provide the protection diodes shown in the circuit diagram. These are provided to limit the voltages appearing across the mixer diode to permissible values.

After completing the construction, align the FET-supply voltage to 6 V. It is possible with the aid of a weak 10 GHz signal for the matching to the mixer diode to be optimized. After this, the transceiver is ready for operation.

5. REFERENCES

(1) Jirmann/Krug:
The Dielectric Resonator;
A Miniature Component for Realizing Stable Microwave Oscillator and Microwave Filters
VHF COMMUNICATIONS 15,
Edition 4/1983, pages 194–201

(2) A. Meier, DC7MA:
Quadrature Demodulators
VHF COMMUNICATIONS 11,
Edition 3/1979, pages 170–173

Horst Burfeindt, DC 9 XG

A SSB Transmit Mixer and Linear Amplifier for 3456 MHz

A 9 cm transmitter is to be described that converts SSB-signals from 144 MHz to 3.456 GHz with the aid of a varactor mixer. This is followed by two, identical amplifier stages equipped with YD 1060-tubes, and provides an output power of 12 W. A version of this transmit mixer is under test for the 6 cm band, and will be published later.

1. VARAKTOR POWER MIXER EQUIPPED WITH BXY 28

This transmit mixer equipped with a varactor diode uses an interdigital filter principle and exhibits a simple construction (see **Figure 1**), and a relatively high output power. One advantage over wideband hybrid mixers is the suppression of the local oscillator and image frequencies. The output power of the mixer is suitable for portable operation.

The low-impedance matching of the diode using a thick center finger is decisive for obtaining a high efficiency. This finger is bypassed for higher frequencies using a mica disk, as shown in **Fig. 2** (approx. 70 pF). The matching at 145 MHz is made with the aid of a Pi-filter. This filter is constructed on silver-plated brass plate which is screwed to the base plate of the mixer case (see **Figure 3**).

The operating point adjustment of the varactor diode is made with the aid of a 100-kΩ-

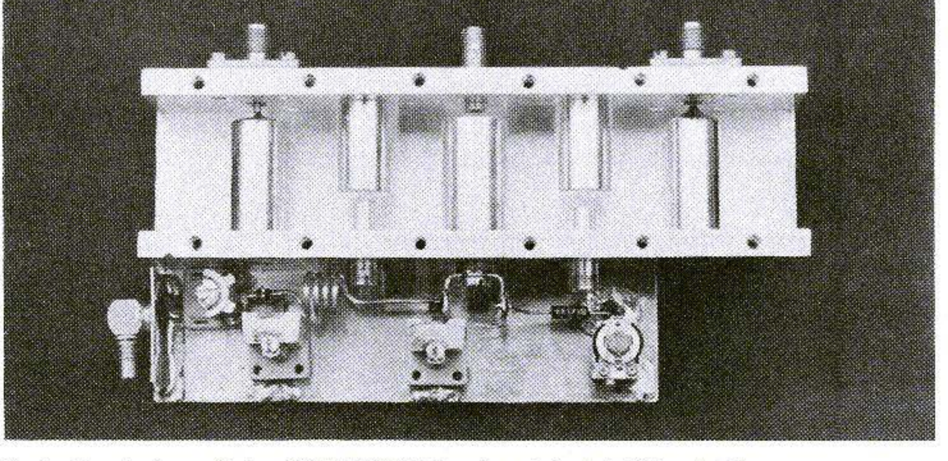

Fig. 1: Varactor transmit mixer 144 MHz / 3456 MHz using an interdigital filter principle

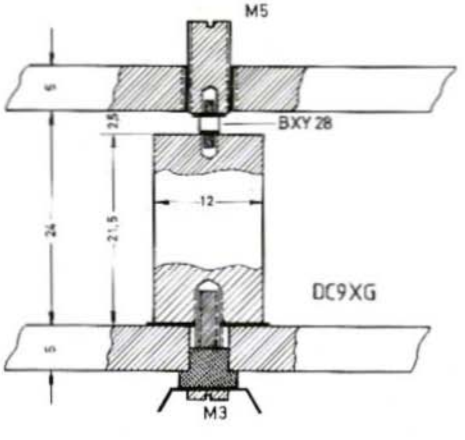

Fig. 2:
The center finger of the interdigital filter supports the varactor diode BXY 28

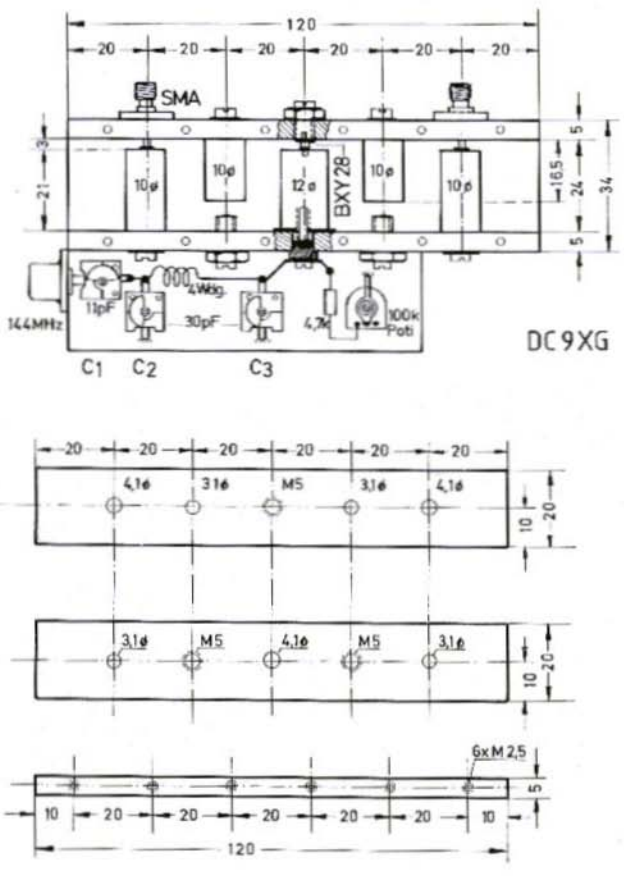

Fig. 3:
Construction and dimensions of the individual parts of the varactor mixer.

potentiometer. The required value depends on the local oscillator and 145 MHz drive levels.

A 6 dB-attenuator should always be provided between the 2 m-transmitter and the mixer. The input impedance of the varactor is very complex at the RF-side, and is very dependent on the drive levels.

1.1. Measured Values

The output power at 3456 MHz amounted to 0.8 W at a local oscillator power of 1.6 W at 3312 MHz. The 3 W-output signal from the 144 MHz transmitter was passed through a 6 dB-attenuator where it was reduced to approx. 0.8 W. The suppression of the local oscillator signal amounted to 18 dB; the image frequency has a rejection of 24 dB.

1.2. Components

Side pieces:	Flat brass (mm): 20 x 5 x 120
Cover:	2 mm brass plate: 34 x 120
Pi-filter plate:	0.5 mm silver-plated brass plate, 30 x 95
Resonators:	Round brass: 10 and 12 mm dia.
Tuning screws:	M5 x 18 mm, fine thread (0.5 mm)
Connectors:	SMA-square flange with PTFE collar
Trimmers:	Milled air-spaced trimmers
Inductances:	6 mm dia.; 4 turns; 1 mm silver-plated copper wire
Mica disk:	12.5 mm dia. (insulating disk for power diodes)
Insulated feed-through:	Nylon or PTFE 4 or 6.4 mm dia.
Diode:	Varactor BXY 28 (Philips)

2. 3456 MHz AMPLIFIER EQUIPPED WITH YD 1060

The power amplifier for 3456 MHz is built up in a coaxial manner (see **Figure 4**). The anode cavity operates in a $\lambda\ ^3/_4$ mode at this frequency and the cathode circuit is operated in a $\lambda\ ^5/_4$ mode.

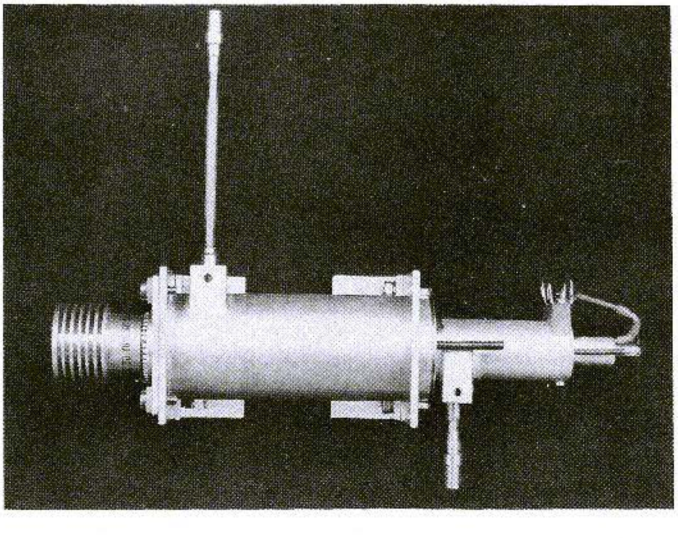

Fig. 4: 3456 MHz-amplifier with the input facing down, and the output (semirigid cable) facing upwards

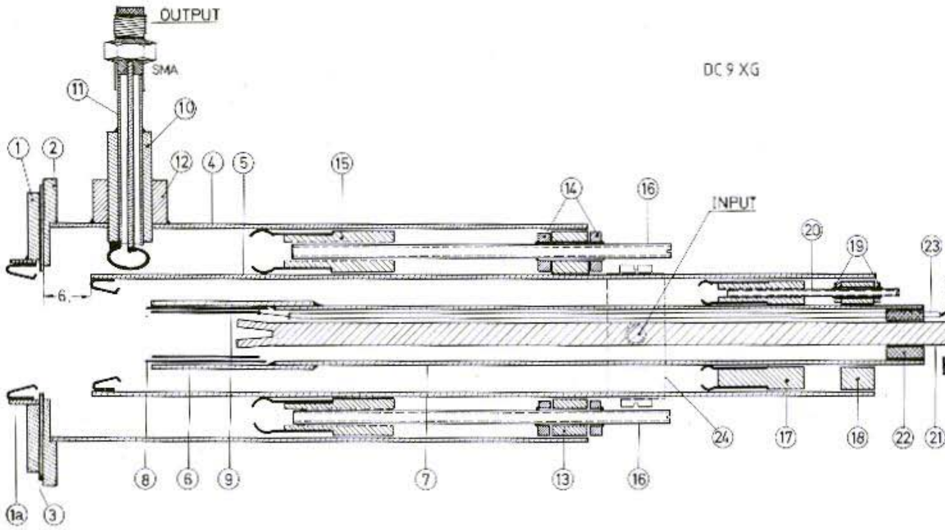

Fig. 5: Coaxial amplifier for 3456 MHz using a YD 1060

The anode and grid circuits are arranged on the same side **(Figure 5)**, which results in a shorter constructional length. The tuning is also carried out on this side, which means that the tube can be easily exchanged.

The coaxial resonators are made from thin brass tube. Bent contact material is used for the contact between these resonators and the grid and anode. The grid is grounded. A home-made cathode capacitor is used for DC-blocking.

The drive power is injected galvanically in the vicinity of the tuning plunger. The output coupling is made inductively with the aid of a loop in the upper part.

The large-signal gain of this amplifier is greater than 10 dB (!), and provides an output power of 12 W. However, the anode current amounts to 140 mA at an operating voltage of 400 V, which is no longer permissible according the specifications of the manufacturer.

If this stage is used as power-mixer, one will obtain an output power of approximately 1 W at 3456 MHz with a local oscillator power of 400 mW at 3312 MHz.

2.1. Detailed Construction

The anode and cathode plungers (15) and (17), as well as sealing rings (13) and (18) for the anode and cathode cavities are all lathed components. These, and other parts, are given together with all dimensions in **Figures 6 and 7.**

Anode Cavity

The anode plate (1) and anode support plate (2) were cut by the author from 2 mm thick brass plate using a metal circular saw.

The support plate (2) has been countersunk to a depth of 1 mm in order to accept the 30 mm anode tube (4) to which it is centered.

10 mm flat brass of 35 x 35 mm is suitable for the anode output coupling mount.

The brass block is drilled through using the 30 mm countersink and then cut in a suitable manner so that the two output coupling mounts result.

Before soldering together, the anode support plate (2), the output coupling mount (12), and the anode tube (4) should be cleaned with

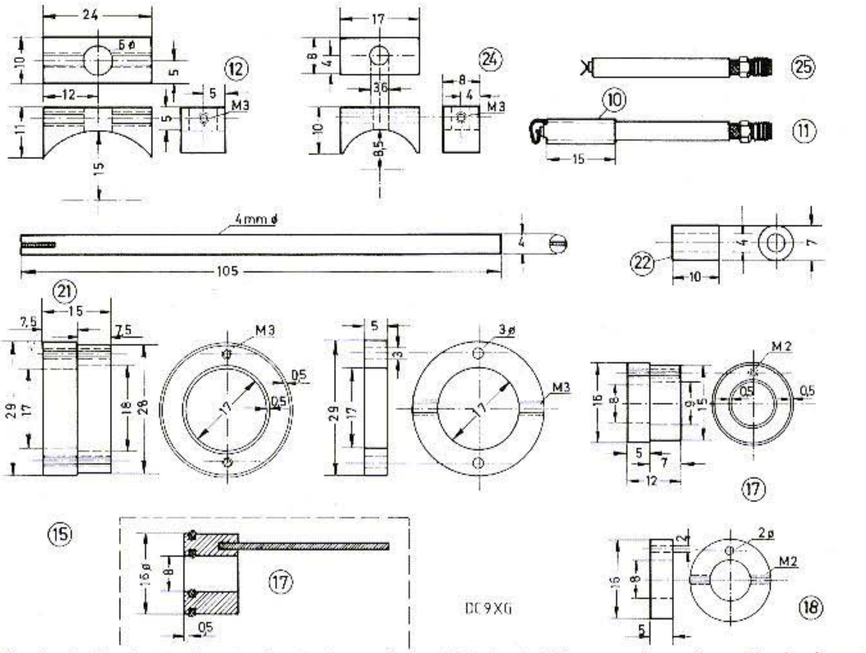

Fig. 6: Lathed parts, input and output coupling; within dashed lines: **an alternative cathode plunger**

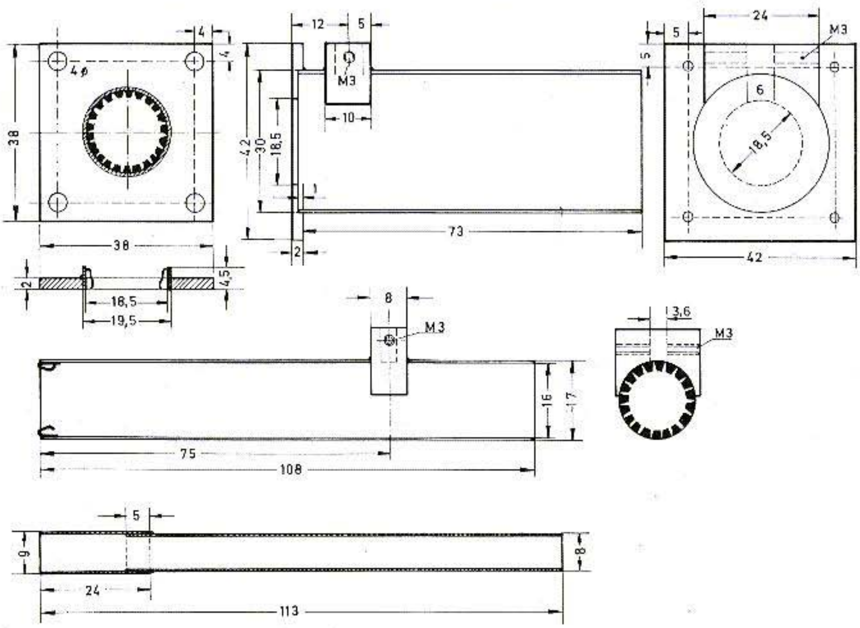

Fig. 7: Anode cavity, grid and cathode tubes

steel-wool. Parts (12) and (4) are provided with a thin solder coating and with a M5-screw which is pushed through the output coupling hole. The three parts are soldered together using soft solder and a gasburner.

Anode Plate

The anode plate (1) and the 4.5 mm high collar (1a), as well as the bent contact material are soldered together with 1 mm colophonium solder on the plate of an electric oven.

A 4.5 mm length of brass-tube is required for the collar (1a). The author used a piece of 30 mm anode tube material. A piece can be cut out using wire cutters. This open ring is then formed so that it fits into the 19.5 mm hole. The inside of the collar, which has been solderplated, and the contact should be provided with solder lacquer. A defective tube, or an electrolytic capacitor with a diameter of 15 mm, can be used during the soldering process to ensure a constant pressure.

Grid Tube

The manufacture of the grid tube (5) and input coupling mount (24) is made in the same manner as the anode cavity.

The brass block of 30 x 18 x 8 mm required for the input coupling mount, is drilled through using a 17 mm countersink, and then cut. The grid tube and the bent contact strips are provided with a thin layer of solder and subsequently sprayed with soldering lacquer. A defective YD-tube or a piece of tubing can be used during the soldering process to ensure the correct pressure.

Cathode Tube

A 7 mm drill is placed in the longest of the 8 mm tubes (7) for orientating the 24 mm long cathode tube (6). A short piece of 8 mm tubing, which is placed in the cathode connection, ensures an exact fit. The overlap between (6) and (7) amounts to 5 mm.

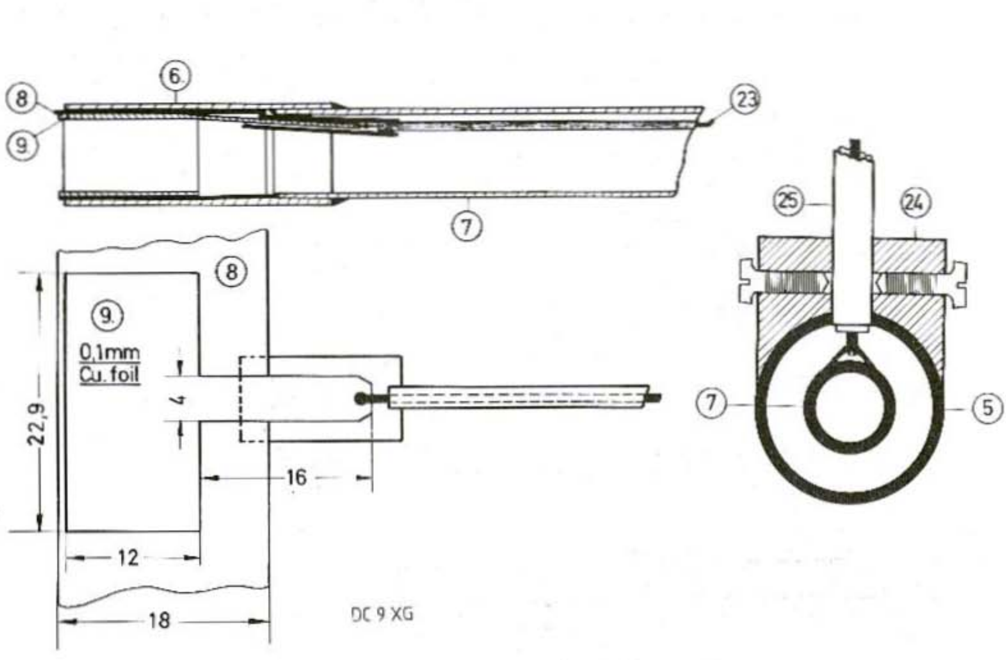

Fig. 8: Cathode connection, cathode capacitor, and RF-input coupling

Cathode Capacitor

A 0.1 mm thick copper foil (9) is cut as shown in **Figure 8** and is wound around the cathode shaft of the tube. Several layers of Kapton-, PTFE, or similar foil (8) are used as dielectric (maybe even Sellotape would be suitable).

The outer diameter of this capacitor should just fit into the 9 mm cathode tube (6). For those readers that would like to exchange the tube easily, it is advisable for them to glue the copper foil, dielectric, and brass tube with a small amount of dual-component glue.

Cathode Feed

A 0.5 mm PTFE insulated copper wire (23) is used for the cathode supply. This wire is soldered to the 4 mm wide connection tab of the copper foil. The tab is provided with a layer of Sellotape on both sides for insulation.

Heater Voltage Contact

The 4 mm diameter brass piece (21) is cut in the form of a cross and pulled out slightly. Two insulated plexiglas pieces center the heating contact. A continuous fit can be guaranteed by pouring in warmed dualcomponent glue between the cathode tube and heater voltage contact.

Anode and Cathode Plungers (15) and (17)

The plunger and contact material are provided with a thin layer of solder. The external part of the contact material is pressed on using several turns of wire.

A short piece of grid or cathode tubular material is used to ensure a good pressure of the internal contacts. The tubes are increased on one side by providing several layers of 5 mm wide Sellotape. The film side then depresses the contact material onto the inside of the plungers. One must pay attention that the contact fingers are protected when soldering with the aid of a gas-burner.

Alternatively, it is possible for the cathode plunger (17) to also be made without using expensive contact material (see **Figure 6**). Using a lathe, the front side of the plunger is provided with grooves on the inside and outside, and these are filled with silver-plated stranded wire (such as the screening of thin coaxial cable).

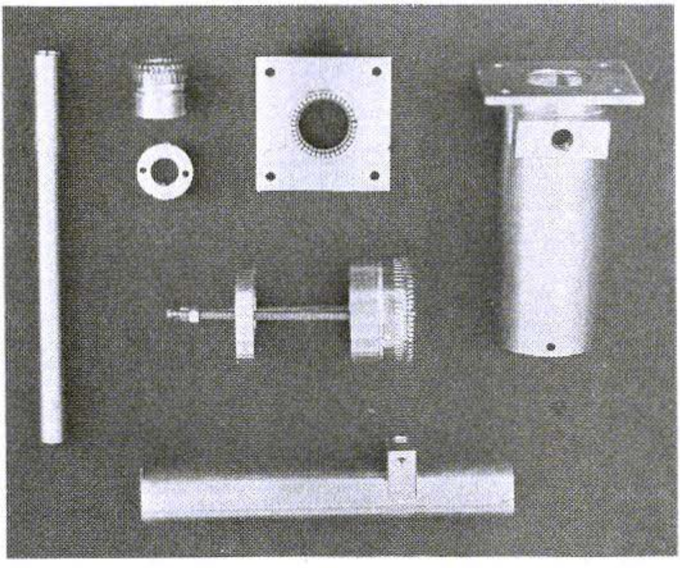

Fig. 9: Individual parts of the 3456 MHz amplifier after soldering together

RF-Input and Output Coupling

Semirigid cable of 3.6 mm in diameter equipped with SMA-connectors is required for the input and output coupling (25) and (11). Drilled spacer bushings (10) are soldered to the copper material in order to ensure that the cable is not bent by the clamping screws. The 2 mm wide output coupling loop is made from 0.5 mm brass plate.

The galvanic RF-injection (25) to the cathode tube (7) is in the form of a contact (bronze plate).

Figures 9 and 10 show the completed parts for one amplifier stage soldered together, or partly mounted.

2.2. Alignment

Cathode Circuit

The cathode cavity is aligned with the aid of a signal source to 3456 MHz. The shortcircuit plunger should be aligned for maximum cathode current. With some tubes, it was necessary for the input coupling to be made capacitively. The bronze plate of the contact is then used as one plate of the capacitor.

Anode Circuit

The inductive output coupling is very critical! It is made by turning and inserting the coupling loop into the anode cavity. There is a directional characteristic. The maximum ouput power should be determined by rotating the loop by 180°.

2.3. Interconnection and Measured Values

The author's 3456 MHz-transmitter **(Figure 11)** has three stages. The described varactor transmit mixer operates in its low-power range

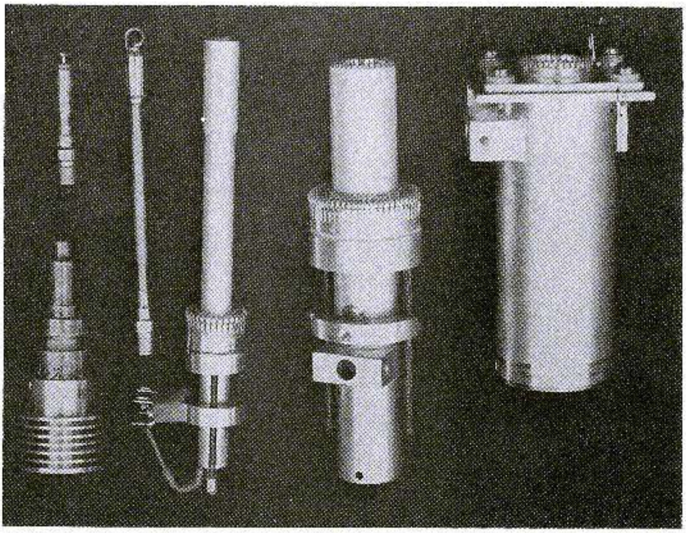

Fig. 10: 3456 MHz-PA together with YD 1060 ready for assembly

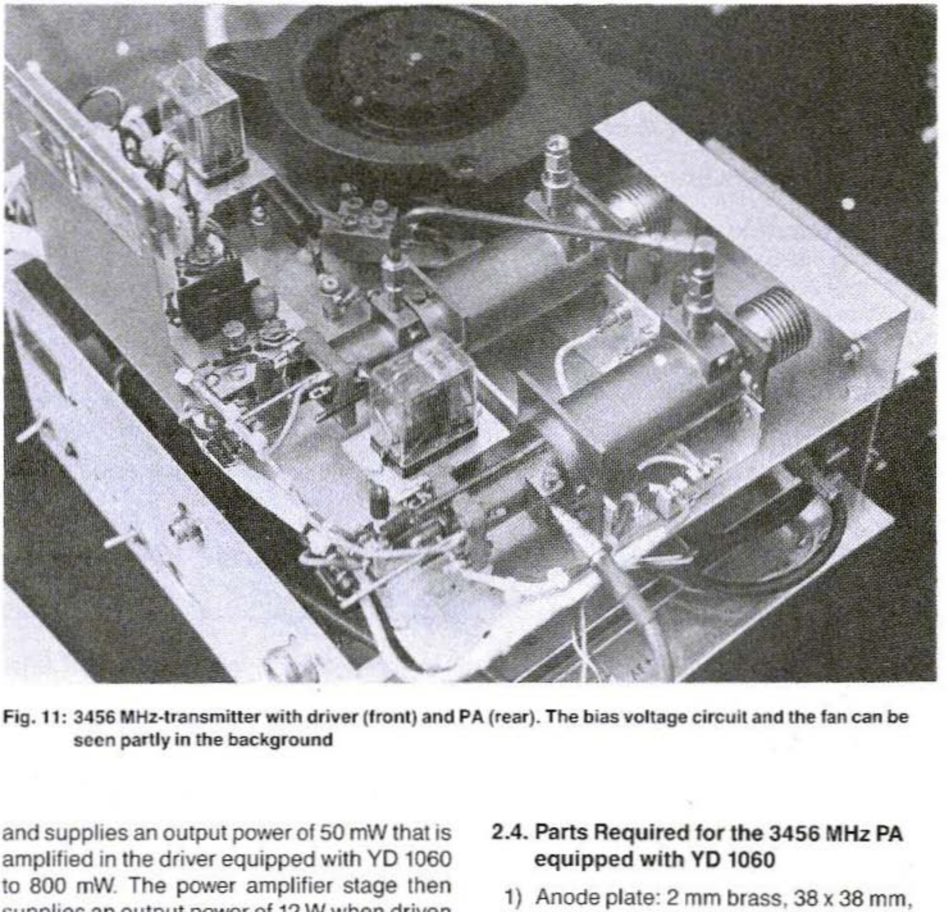

Fig. 11: 3456 MHz-transmitter with driver (front) and PA (rear). The bias voltage circuit and the fan can be seen partly in the background

and supplies an output power of 50 mW that is amplified in the driver equipped with YD 1060 to 800 mW. The power amplifier stage then supplies an output power of 12 W when driven with 800 mW. The quiescent anode current of both stages amounts to 20 mA.

The operating point adjustment is made with a circuit similar to that described by LA 8 AK in (1). The anode voltage of 400 V is electronically stabilized. The gain is dependent on the anode quiescent current. No advantages were found on increasing the anode voltage further to 450 or 500 V.

All stages operate very stabily, and no tendency to oscillation was found. The high output power remains constant during SSB-operation. The alignment and the coupling need not be retuned.

2.4. Parts Required for the 3456 MHz PA equipped with YD 1060

1) Anode plate: 2 mm brass, 38 x 38 mm, hole 19.5 mm dia.
2) Anode support plate: 2 mm brass, 42 x 42 mm, hole 18.5 mm dia.
3) Anode capacitor: Dielectric: Mica, PTFE, Kapton, or similar foil 40 x 40 mm
4) Anode tube: Brass, 30 mm dia., 0.5 mm thick, 74 mm long
5) Grid tube: Brass 17 mm dia., 0.5 mm thick, 108 mm long
6) Cathode tube: Part 1, brass, 9 mm dia., 0.5 mm thick, 24 mm long
7) Cathode tube: Part 2, brass, 8 mm dia., 0.5 mm thick, 94 mm long
8) Cathode capacitor: Dielectric: Kapton, or possibly Sellotape
9) Copper foil, 0.1 mm thick

10) Drilled spacer bushing for the RF-output coupling, 6 mm dia., 10 mm long
11) 3.6 mm semirigid cable with coupling loop
12) Anode output coupling: Material: 10 mm brass, 35 x 35 mm
13) Anode cavity sealing ring: Material: brass
14) Rounded M3-brass nuts
15) Anode plunger: Round brass, 29 mm dia.
16) 2 threaded bolts – M3 x 60 mm
17) Cathode plunger: Round brass, 16 mm dia.
18) Cathode cavity sealing ring
19) Brass nuts: M2
20) Threaded bolt: M2 x 30 mm
21) Heater voltage contact: Round brass, 4 mm dia., 105 mm long
22) Insulating tube (plexiglass), 7 mm dia., 10 mm long
23) Galvanic cathode connection: PTFE-insulated wire, 0.5 mm dia.
24) Cathode input coupling mount: Material: 8 mm brass, 30 x 18 mm
25) RF-Input Coupling: 3.6 mm semirigid cable, possibly provided with a drilled-out spacer bushing

Contact strips: Suitable contact strips for the 2C39/YD range of tubes

3. REFERENCES

(1) Jan M. Nøding, LA8AK:
Bias Voltage Circuit for Tubes of the 2C39/3CX100 Families
VHF COMMUNICATIONS 14, Edition 3/1982, pages 148 – 149

Erich Stadler, DG 7 GK

Using Smith Diagrams

In RF-technology, one often displays real and reactive impedances as a function of frequency in the form of a "focus". Figure 1 shows a typical example of this with an RF-transistor TDA 1087, and Figure 2 with a HB 9 CV-antenna. This article is to describe how to read Smith diagrams, and how to use them to advantage.

Every electronics technician knows that a series connection of real and reactive impedances can be shown graphically as two arrows that are perpendicular to another **(Figure 3)**. If this is to be displayed in a more exact manner mathematically, these two vectors should be inserted into a system of coordinates where the real impedances are inserted

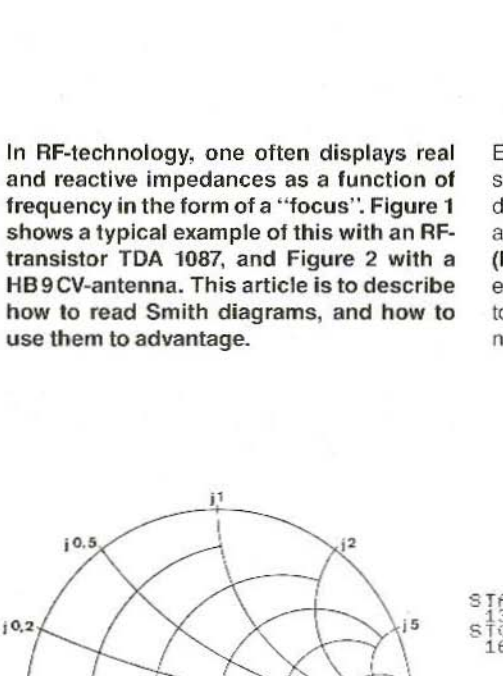

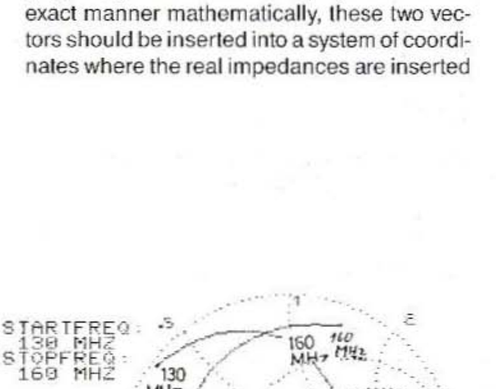

Fig. 1: Input impedance of a TDA 1087 as locus in a Smith diagram

Fig. 2: Impedance locus of a HB9CV antenna for the 2 m band

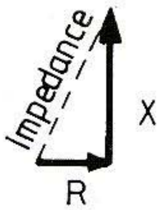

Fig. 3: Real and reactive impedance

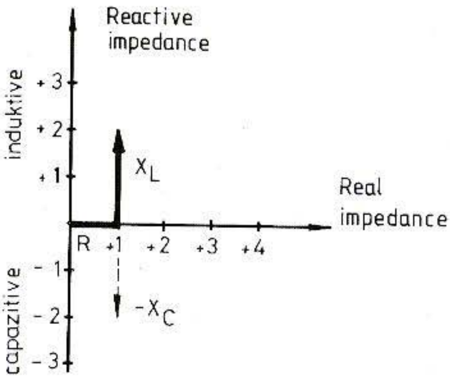

Fig. 4: Real and reactive impedances in a coordinate system

to the right, and the reactive impedances vertically. A vector pointing upwards (positive sign) represents an "inductive reactive impedance", and a vector pointing downwards (negative sign) shows a "capacitive reactive impedance" **(Figure 4).**

This impedance plane has the disadvantage that it must be extended infinitely if it is to display all possible impedance conditions, such as the infinite impedance present under non-load conditions.

This problem can be solved by "bending" the vertical coordinates in the impedance plane **(Figure 5, left)** to form circles. Of course, the vertical axis must form the outer circle **(Figure 5, center);** the reactive impedance values $+\infty$ and $-\infty$ are in the "finite" then.

This is where the outer circle **(Figure 5, right)** intersects the horizontal axis. The consequence of this is that the real-impedance axis is no longer linearly scaled. Here, also the impedance value ∞ comes into finite values and meets the other two infinite points at the right.

The bending process also has an effect on the horizontal coordinates which are in the form of sectors. With increasing inductive or capaci-

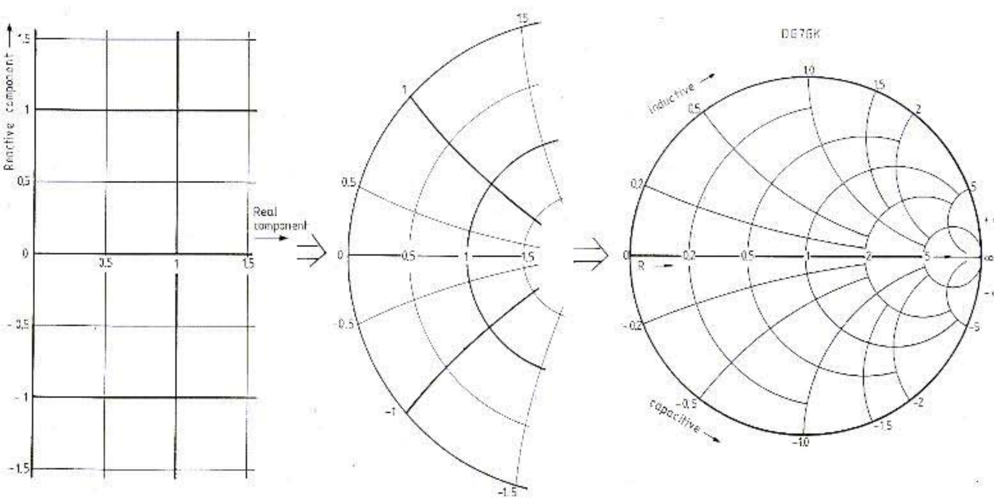

Fig. 5: Transition from rectangular coordinate system to Smith diagram

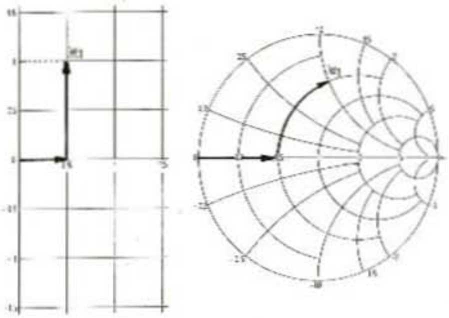

Fig. 6a:
Series connection of real and reactive component: Real component = 0.5; reactive component = 1.0. "+" means "inductive".

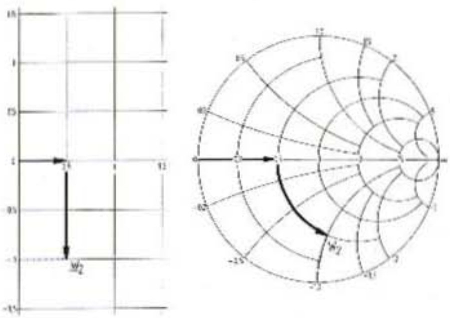

Fig. 6b:
Series connection:
Real component = 0.5;
reactive component = −1.
"−" means "capacitive".

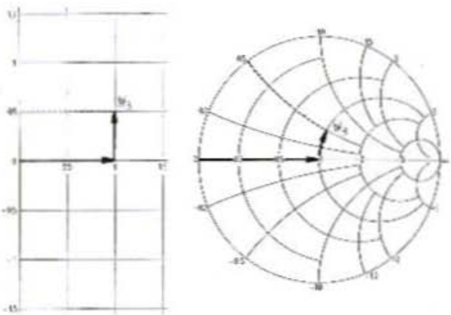

Fig. 6c:
Series connection:
Real component = 1.0;
reactive component = +0.5

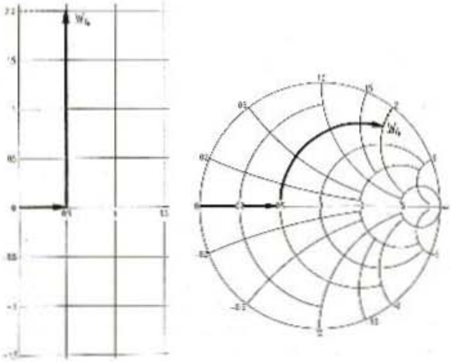

Fig. 6d:
Series connection:
Real component = 0.5;
reactive component = +2

tive reactive impedance they become continuously shorter and are shifted more and more to the infinite point. The whole rectangular system of coordinates in the impedance plane with its straight coordinates is thus transposed to a curved coordinate system that fills the inside of a circle. Only the right angles (intersections of originally horizontal and vertical coordinates) remain intact during the "bending" process.

It is advisable to practise by inserting the real and reactive impedances in the left half of the Smith diagram, before attempting to enter into the area where the originally vertical coordinates transpose into the horizontal and finally reverse the direction, or where the originally horizontal coordinates reverse their direction. Several points are given in **Figure 6**a to d ($\underline{\mathbf{W}}_1$, $\underline{\mathbf{W}}_2$, $\underline{\mathbf{W}}_3$ and $\underline{\mathbf{W}}_4$). The associated reactive and real impedance components must be taken from the bent coordinates. $\underline{\mathbf{W}}_4$ has an extremely high reactive component, which means that this point has exceeded the vertex of the circle. The insertion and extraction of data in this area is very complicated. In this range in the vicinity of infinite values, the coordinates are very close together, which means that only a few can still be inserted. Intermediate values must be read off or inserted by interpolation.

On studying Figure 6a to d as well as 1 and 2, one could assume that only impedances in the order of 0.1 Ω to approximately 2 Ω are suitable for the diagram. This is, however, not the case in practice, since only standard values are inserted into the diagram. This **standardization** allows the same diagram to be used universally.

The standardization process is now to be shown with the aid of an **example:** A series circuit exhibiting a real impedance of 20 Ω and a reactive impedance of 40 Ω is to be inserted into the diagram. If standardization were not used, it would be necessary to insert the value 20 or 40 virtually at ∞, which would be useless due to the inaccuracies. Standardization on the other hand means that it is necessary to **divide** the given impedance values by a suitable, so-called standardizing impedance Z_{st}.

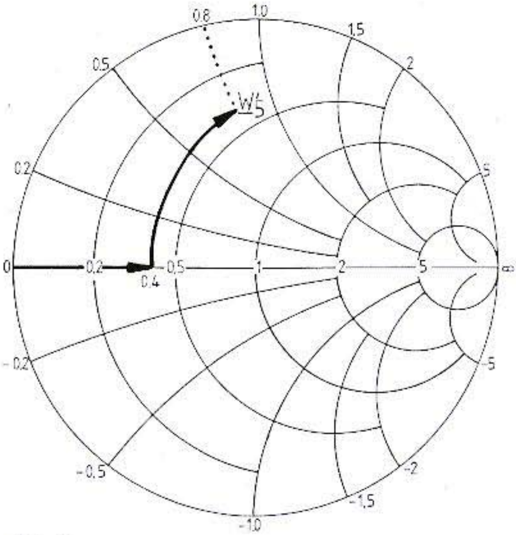

Fig. 7:
Real impedance = 20 Ω;
reactive impedance = 40 Ω
Standardized: Real component = 0.4
Reactive component = 0.8 } **= $\underline{\mathbf{W}}'_5$**

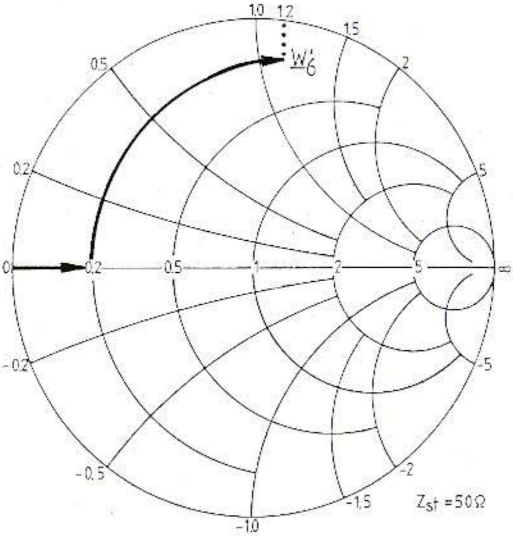

Fig. 8:

$\underline{\mathbf{W}}_6$ is standardized:	**Real component = 0.2**
	Reactive component = 1.2
After destandardization	**Real component = 10 Ω**
	Reactive component = 60 Ω

In our case, we select a Z_{st} of 50 Ω. This results in a standardized real component of 20 Ω/50 Ω = 0.4; and a standardized reactive component of 40 Ω/50 Ω = 0.8.

The standardized values 0.4 and 0.8 are inserted into the diagram **(Figure 7)**, and it can be seen that the resulting point $\underline{W}'_5$ is located very favourably. In our example, 0.4 and 0.8 are numerical values representing the type of an impedance, with 1 as unit.

If one reads such numerical values out of the diagram, one must know the value of the standardizing impedance applied before the entry into the diagram. Another **example: In Figure 8** one will see a point $\underline{W}'_6$ which is to be found on the real-impedance coordinate 0.2, and on the reactive-impedance coordinate 1.2. Since the standardizing impedance Z_{st} = 50 Ω is marked on the diagram, one knows that these values are based on a standardized impedance of 50 Ω. If one wishes to know the actual impedance values, it is necessary to "de-standardize" them.

This is carried out by **multiplying** them with the standardizing-impedance values: The resulting real-impedance value is

$Z = 0.2 \times 50\,\Omega = 10\,\Omega$,

and the actual reactive-impedance is

$X = 1.2 \times 50\,\Omega = 60\,\Omega$.

The values also receive their actual unit "Ω".

In principle, the selection of the standardizing-impedance value can be made freely, however, in practice one is dealing with real and reactive impedances that are to be matched to a certain impedance, such as a source or load impedance. Another application would be to match the characteristic impedance of a transmit antenna to a certain impedance of the feeder cable. If one wishes to use the advantages of the diagram – that is, reading out the value of the return loss of the load or antenna impedance from the diagram, as a function of the source or load impedance – it will be necessary to standardize the diagram to the impedance of the source, that is the source impedance or the impedance of the line. Since an impedance of 50 Ω is usually used in communication technology, it is favorable to select this impedance as standardizing impedance. In Figure 1, an impedance Z_o = 50 Ω was given by the manufacturer. This Z_o is the standardizing impedance which we have designated Z_{st} in this article. Fundamentally speaking, it is always necessary to give the value of the standardizing impedance used when displaying impedances in a Smith diagram!

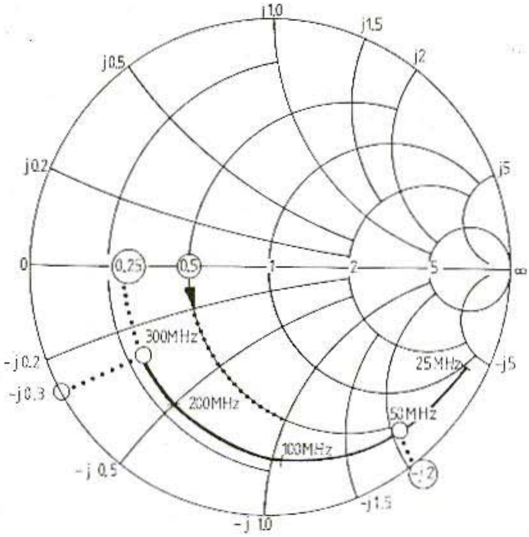

Fig. 9: Determining the input impedance of a transistor with respect to real and reactive component at 50 and 300 MHz

Finally, a further example is to demonstrate once again the reading of Smith diagrams and the de-standardization process in conjunction with the RF-transistor TDA 1087 (Figure 1). This diagram is repeated in **Figure 9**. The **question** is: What is the impedance (real and reactive components) of the transistor at 50 MHz and 300 MHz?

Solution: The 50 MHz-point is to be found on the locus at a real component of "0.5", and a reactive component of approximately "–2" (the factor "j" only shows that it is a reactive and not a real component). The minus-sign means that it is a capacitive reactive component.

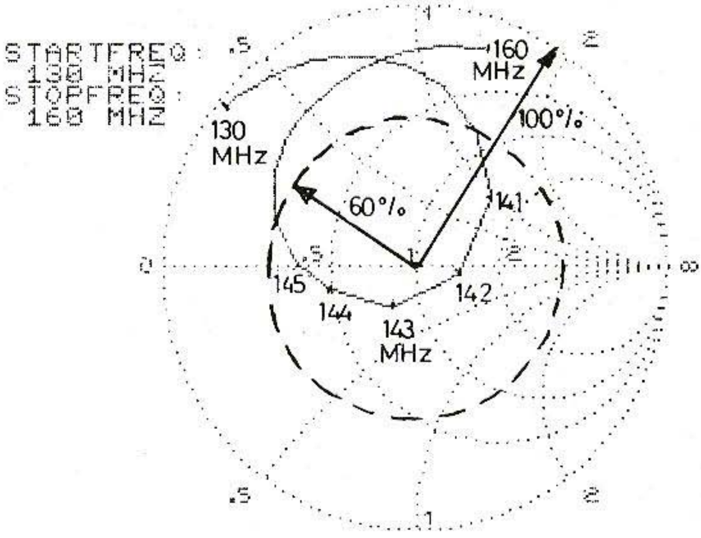

Fig. 10: Locus of an antenna impedance: Return loss circle |r| = 60%

After de-standardizing, the following results at 50 MHz: Real impedance R = 0.5 x 50 Ω = 25 Ω; reactive impedance X_c = −2 x 50 Ω = −100 Ω ("−" means "capacitive"). The 300 MHz-point is to be found on the locus at a real component of "0.25" (estimated) and a reactive component of approx. "−0.3".

After de-standardization, this results at 300 MHz in the following:

Real impedance R = 0.25 x 50 Ω = 12.5 Ω;
reactive imp. X_c = −0.3 x 50 Ω = −15 Ω.

The advantage of the return loss diagram is to be shown together with a HB9CV-antenna. The locus of the impedance of this antenna (Figure 2) is repeated in **Figure 10.** The diagram is standardized to 50 Ω and the antenna is to be connected to a feeder cable of also 50 Ω, which means that it is not necessary to re-standardize the locus. It is now possible to simply determine in which range the antenna does not exceed a certain return loss! However, this requires one more curve in addition to the many other curves already existing in the diagram.

The return-loss limits are indicated by the radial length of a circle whose center is the **geometric** center of the diagram. The radius of the outer circle is used as a reference value, since all impedance values on the outer circle possess a return loss of 100% with respect to the standardizing impedance. If one wishes to mark the range in which the locus contains impedances having a certain return loss with respect to the standardizing impedance of 50 Ω, for instance a return loss for 60%, it is only necessary to form a circle around point 1 (center of the diagram) which has a radius of 60% that of the outer circle.

All impedances that are to be found within this circle will have a return loss of less than 60% with respect to the standardizing impedance, and thus with respect to the impedance of the feeder cable. It will be seen that the antenna is matched to the cable with a return loss of less than 60% in a frequency range of 141 MHz to 145 MHz. If the **voltage standing wave ratio VSWR** is to be read off, this is possible by reading it out of the diagram between 1 and ∞ at the intersection between the appropriate return loss curve and the horizontal axis.

It will be seen that one is able to solve many problems encountered with return loss, standing wave ratio, and matching, without having to carry out complex calculations.

Editors

A 2400 Hz Generator for Synchronization of the METEOR Satellites

The digital storage described by YU3UMV in (1) derives its synchronization from the 2400 Hz subcarrier which is provided by the weather satellites METEOSAT, GOES, and NOAA. This is also supposed to be the case with the Russian METEOR weather satellites, however, only one of their satellites is now transmitting with the standard subcarrier frequency of 2400 Hz. This is the 240 lines/min. satellite operating on 137.120 MHz (originally 137.150 MHz). The subcarriers of the other satellites operating on 137.30 and 137.85 MHz (120 lines/min.) are using a subcarrier of approximately 2500 Hz, which means that they cannot be synchronized correctly by the YU3UMV module and are displayed diagonally across the screen. The following article is to describe an external synchronization source that can be added to the video storage module and connected to the synchronizing input.

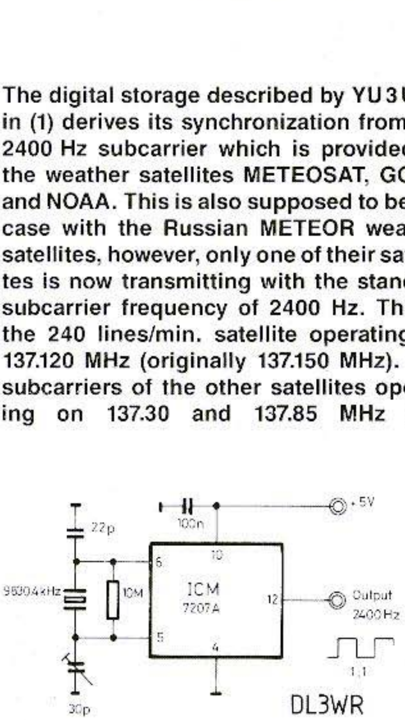

There are several ways of obtaining a frequency of 2400 Hz from a crystal-controlled frequency in the MHz-range by using digital frequency dividers. Two such circuits are shown in **Figure 1.**

DF9RL uses two standard CMOS-ICs: I 1, a 4060, comprises an oscillator and a 512 divider, and I 2 (4518) is a divider that can be programmed by diodes. The latter is set for a division ratio of three so that an overall division ratio of 1536 results. A crystal of 3686.40 kHz is thus required. This small module can also be used for other applications by using other crystal frequencies and/or a different program-

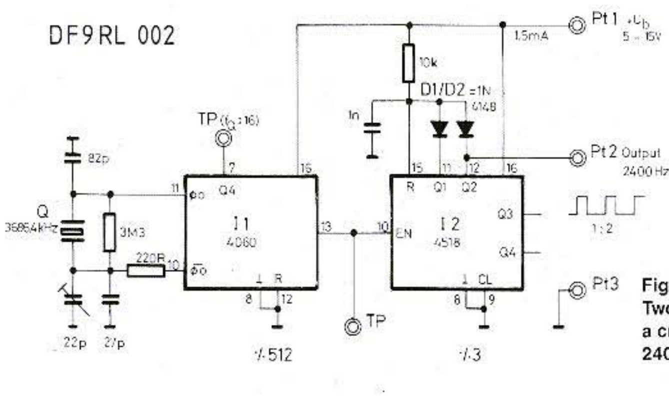

Fig. 1:
Two simple circuits for generating a crystal-controlled frequency of 2400 Hz

ming of I 2. The technical specifications are:
Operating voltage U_b = 5 to 15 V
Current drain I_b = 1.5 mA at 5 V
Crystal frequency = Output frequency x 1536
Keying ratio = 1:2
Crystal: Parallel resonance with 30 pF load

DL3WR uses an IC that was used as drive circuit in the DK1OF 044/045 frequency counter (2). This circuit comprises an oscillator and a divider of 2^{12} (4096). This circuit is very compact and uses a minimum of components. The required crystal operates at a frequency of 9830.40 kHz. The IC has a number of other outputs that are not required for our application. The technical specifications of the circuit described by DL3WR are:

Operating voltage U_b = 5 V (max. 5.5 V!)
Current drain I_b = 0.26 mA (typ.)
Crystal frequency = Output frequency x 4096
Keying ratio = 1:1
Crystal: Parallel resonance with 15 pF load

A small, single-coated PC-board of 55 mm x 45 mm was designed for accommodating the universal circuit DF9RL 002 (**Figure 2**). No PC-board was designed for the DL3WR-circuit, which can be built up on a piece of Veroboard, as shown in **Figure 3**.

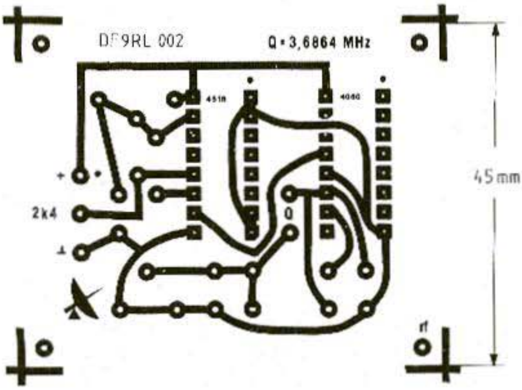

Fig. 2: Single-coated PC-board DF9RL 002

REFERENCES

(1) Matjaž Vidmar, YU3UMV:
A Digital Storage and Scan Converter for Weather Satellite Images
VHF COMMUNICATIONS 14 (1982), Edition 4, pages 194-208

(2) J. Kestler; DK1OF:
A Settable Up-Down Frequency Counter
VHF COMMUNICATIONS 13 (1981), Edition 2, pages 83-94

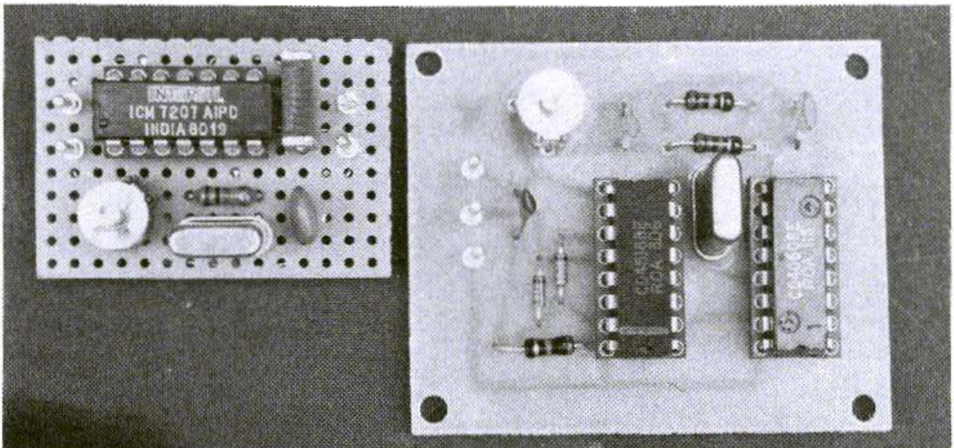

Fig. 3: Two different 2400 Hz sources for synchronizing the YU3UMV video storage for the reception of METEOR weather satellites

VHF communications

Index of Volume 16 (1983)

Dragoslav Dobričić, YU 1 AW

Determining the Parameters of a Receive System in Conjunction with Cosmic Radio Sources

The editors would like to point out that the article (1) written by Guenther Hoch, DL 6 WU, provides an excellent basis for the following considerations. The following article is to describe antenna noise temperature and the "hot-cold noise figure measuring method", to discuss inaccuracies of sun-noise measurements, to introduce cosmic radio sources, and finally to describe measuring methods with the aid of these sources. The diagrams with measured values of the strongest radio sources at 144 MHz and 432 MHz form valuable reference information. A further diagram gives the data for the wider frequency range of 30 MHz to over 10 GHz.

1. ANTENNA NOISE TEMPERATURE

One of the criteria of a receive system is its ability to receive very weak signals: its sensitivity. The sensivity is determined by only two factors:

Antenna gain (G)
System noise temperature (T_{sys})

The system noise temperature comprises the antenna noise temperature (T_a), the cable losses converted into noise temperature (T_{cable}), and the intrinsic noise of the receiver, or preamplifier (T_{rx}). The latter can be calculated easily according to equation 1 from the known noise figure F:

$$T_{rx} = (F - 1) \times 290\ K \qquad \text{(Eq. 1)}$$

In this case, F is used as factor (not in dB). The equivalent antenna noise temperature (antenna temperature) is the noise power received by the antenna, converted to the temperature of a resistor, whose value is equivalent to the radiation impedance of the antenna.

All objects with a temperature higher than absolute zero (0K), radiate electromagnetic waves due to this temperature. This radiation is well known in physics and can be expressed mathematically as "black-body radiation" according to Planck's law.

The antenna temperature is mainly determined by the noise temperature of objects within its beamwidth. If an object radiates noise due to its intrinsic temperature of due to other noise-generating mechanisms, the antenna will receive this noise and a certain noise power will be present at its connections. Since noise power and equivalent noise temperature are dependent on another according to Boltzman's constant, it is possible to express the received noise power as in increase in antenna noise temperature.

The antenna noise temperature has very little dependence on the physical temperature of the antenna itself that can be measured with the aid of a thermometer! The higher the efficiency of the antenna, that is the greater the ratio of radiation resistance to loss resistance, the less will be the dependence.

The received noise power, or the noise temperature of the antenna, does not only depend on the temperature T of the object, but also on how much this object is present in the antenna diagram. In order to calculate this, it is necessary to operate with the space angles of the object (Ω), and the antenna diagram (Ω_A). This is given in equation 2:

$$T_a = \frac{\Omega}{\Omega_A} T \qquad \text{(Eq. 2)}$$

If Ω is equal to Ω_A, or is greater, this will mean that the antenna will only "see" the object radiating with temperature T; and the antenna noise temperature will be equal to the temperature of the object:

$$T_a = T$$

However, all practical antennas have unwanted lobes and a finite front-to-back ratio. If these are not suppressed considerably, the antenna will receive additional noise power with them. In the case of conventional antennas with beamwidths of less than 25° in both planes, a rule of thumb is given in (2) that takes the effect of unwanted side and back lobes into consideration:

$$T_a = 0.82\, T_{sky} + 0.13\, (T'_{sky} + T_e) \qquad \text{(Eq. 3)}$$

T_{sky}: Mean value of the equivalent noise temperature of space within the main beam.
T'_{sky}: Mean value of the equivalent noise temperature of space within the side lobes.
T_e: Effective noise temperature of the earth (290 K).

Equation 3 is only valid for antennas that are facing towards the sky; it then provides good results.

2. THE HOT-COLD METHOD

One of the most accurate methods of determining the noise temperature of a receiver is the so-called hot-cold method. This is achieved by connecting a resistor to the input of the receiver that has an identical value to the (transformed) radiation impedance of the antenna (usually 50 Ω), and varying its temperature over the widest possible range. The intrinsic room temperature of 290 K is usually used as "hot" temperature, and the "cold" temperature is that of liquid nitrogen (77 K), into which the resistor is placed.

If the noise power ratio Y that occurs between these two temperatures is measured at the receiver output, it is easily possible to calculate the equivalent noise temperature of the receiver in a very accurate manner:

$$Y = \frac{T_h + T_{rx}}{T_c + T_{rx}}$$

$$T_{rx} = \frac{T_h - YT_c}{Y - 1} \qquad \text{(Eq. 4)}$$

Y = Noise power ratio
T_h = "Hot" temperature
T_c = "Cold" temperature

The described hot-cold method can be varied by changing the noise temperature of the antenna instead of the temperature of the connected resistor. This is achieved by pointing the antenna towards the hot sun, and then to a cold point in the sky. The factor Y at the receiver output is measured for these two positions. If the antenna noise temperature T_a is known for these two positions, it is possible together with the antenna gain to calculate the noise temperature of the receive system T_{sys}, or vice versa. The problems involved herewith are to be discussed in the following sections. This is described in detail in (1).

2.1. Accuracy Problems in Conjunction with Solar Noise Measurements

If solar noise is to be used for measurements, it it necessary to know the solar flux S of the Sun. This possesses large fluctuations in dependence of solar activity (1).

On the other hand, the influence of the sky around the sun that is still "seen" by the antenna, is very low since solar noise is so high in comparison. It is only in December and January when the sun is located in front of the galactic center that the noise radiation around the sun can falsify the measurement.

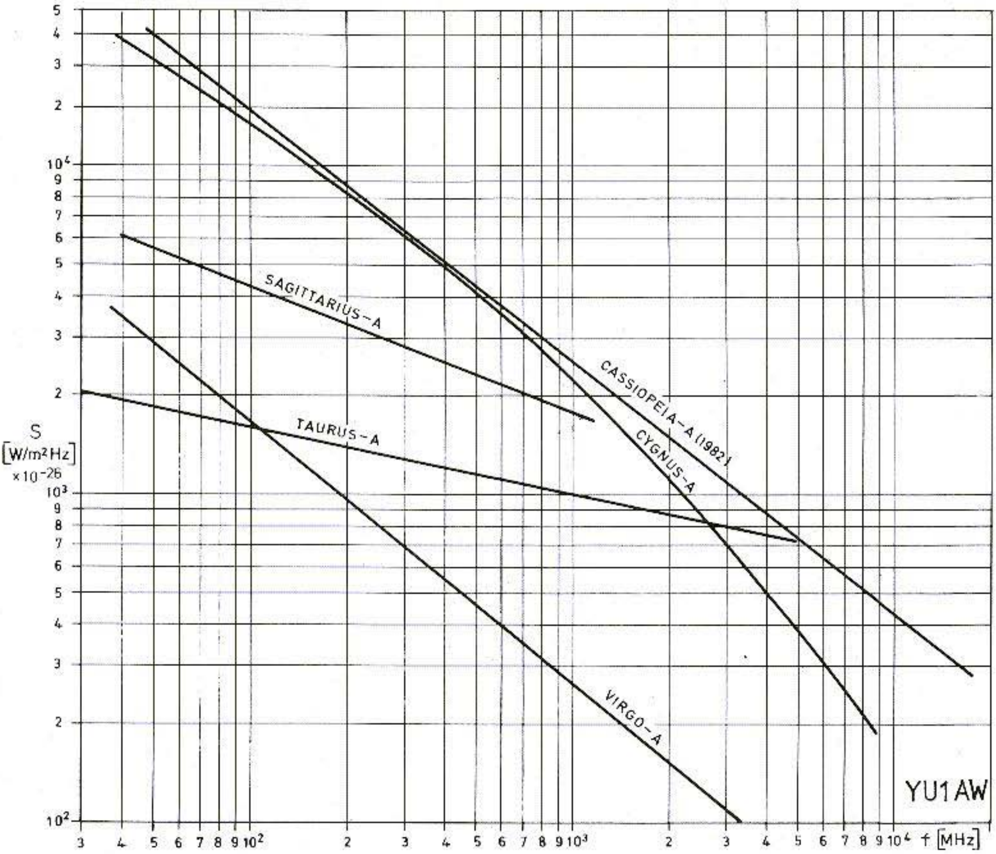

Fig. 1: Noise flux S (× 10^{-26}) of the strongest radio sources (excluding the sun) over the frequency range of 40 to 10000 MHz

Galactic radio sources on the other hand, provide a very much lower, but considerably more constant flux. This means that they can be used instead of the sun to solve problems of inaccuracy. However, their size is so minute in comparison to the beamwidth of conventional antennas, that they represent point sources. The noise temperature of the sky around the radio sources therefore often has a considerable effect on the noise temperature of the antenna. **In order to avoid considerable measuring errors, it is necessary to consider the sky noise around the radio source. This is the reason why one will obtain such inaccurate – or even false – results when the solar noise measuring method is used unchanged with other cosmic noise sources!**

3. GALACTIC RADIO SOURCES

We know the galaxy to which our solar system belongs as "Milky Way". It comprises an immense number of stars, and new stars appear and old stars disappear all the time. These processes are especially frequent in the central regions of the approximately lens-shaped Milky Way and for this reason a relatively very strong noise arrives at the earth from this direction that covers virtually the whole radio spectrum. In addition to this diffuse radiation, there are descrete sources, so-called radio stars, with very strong radiation. The strongest are Cassiopeia-A and Taurus-A. These two radio sources are the remains of Supernova explosions. When viewed through an optical telescope, they are seen as foggy areas, and are therefore called "Nebulars".

There is an infinite number of other galaxies outside our Milky Way, in which enormous processes are taking place, and therefore transmit considerable radiation. These are known as "Radio-Galaxies" and the strongest in the northern hemisphere are Cygnus-A und Virgo-A.

A very strong radio source is located in the core of the Milky Way: It is Sagittarius-A, and is possibly the active core of our galaxy.

Figure 1 shows the noise flux S of the previously mentioned, strong radio sources as a function of the frequency. The curve shows the astrophysisists that the nature of the radiation is not thermal, but is dependent on synchrotron processes (spiral-shaped movements of very fast electrons in strong magnetic fields).

4. SKY TEMPERATURE AROUND THE RADIO SOURCES

As was previously mentioned, the accuracy of the hot-cold method using cosmic radio sources is dependent on the exact knowledge of the mean noise temperature around these radio sources. For this reason, noise power profiles were measured around all the previously mentioned strong radio sources, and a systematic calculation of the mean values was made.

During this process, we soon found that the beamwidth of the main lobe must be taken into consideration, since a different temperature mean value will result for each beamwidth due to the non-constant distribution of the temperature around the sources.

Therefore, the sky temperature was determined as a function of the antenna beamwidth, in steps of 1 dB antenna gain. In the case of the 144 MHz amateur band, a beamwidth range of 25° to 10° was selected which corresponds to gain values of 18 to 26 dB_i. Measured values of the sky temperature were available for 136 MHz and 160 MHz. They were interpolated to obtain values for 144 MHz.

We then noticed that small sky areas, spaced several 10 degrees, are present in the vicinity of the radio sources Cassiopeia and Cygnus, and partly also near Taurus, that have a higher temperature than the direct vicinity of these sources. If one points his antenna simply to the highest noise amplitude, one will obtain false results since one will then be pointing to a position somewhere between the radio source and the "hot" part of the sky. Logically, antennas of differing gain (beamwidth) will be pointing to slightly different directions when aligned for maximum noise level. We have agreed to accept this directional error.

After taking all these things into consideration, very accurate data was obtained for the mean sky temperature around the previously mentioned radio sources, and for the various beamwidths of the antennas. The diagram for T_{sky} at 144 MHz is given in **Figure 2.** In order to make the diagram more usable, the antennas gain in dB_i (isotropic radiator) is also given.

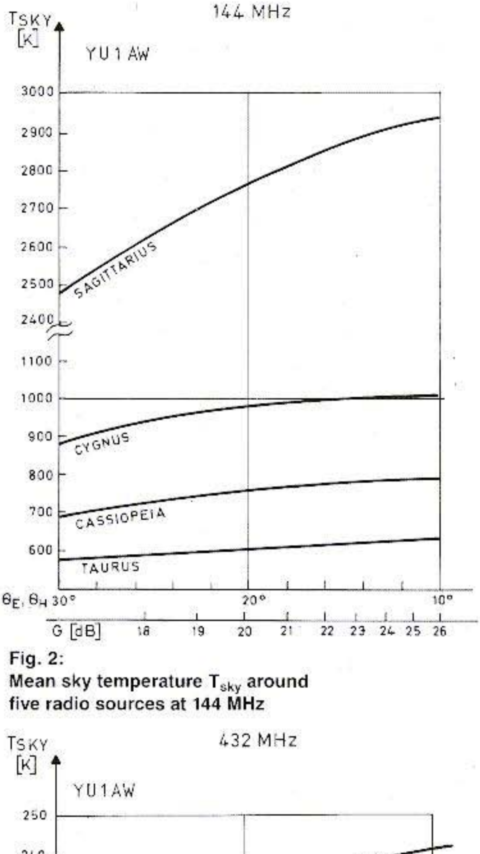

Fig. 2:
Mean sky temperature T_{sky} around five radio sources at 144 MHz

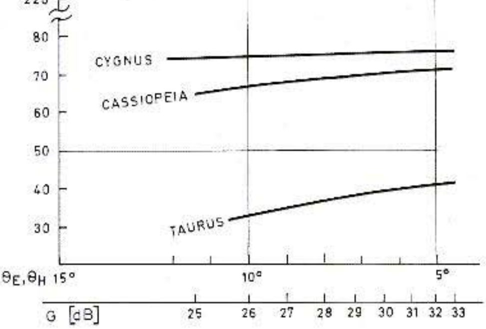

Fig. 3:
Mean sky temperature T_{sky} around five radio sources at 432 MHz

The same process was also made for the 70 cm band, only that the beamwidths were in the order of 10° to 5°, corresponding to a gain of 26 to 32 dB_i. The interpolation for 432 MHz is based on measured values for 400 and 480 MHz. The results are shown in **Figure 3.**

5. DETERMINING THE TEMPERATURE OF THE "COLD" SKY

The knowledge of the temperature of the "cold" points in the sky are just as important as the temperature of the sky around the radio sources. Careful interpolations had been carried out for this, especially for two different "cold" areas of the sky:
In constellation Leo (α = 09:30; δ = 40°) and in constellation Aquarius (α = 22:30; δ = 0°)

The coldest points in these areas have temperatures of 195 K, or 275 K at 144 MHz. Mean temperature values as a function of the various antenna beamwidths were found for both "cold" areas. In the case of 432 MHz, the difference between Leo and Aquarius is only 5 K, which means that both areas can be classed as being equally cold, namely 20 K.

With the aid of the Tailor-equation (Eq. 3) we determined the temperature of a directional antenna (T_{acs}), pointing towards this position, from the temperature of the cold sky (T_{cs}). In this case, the mean value of the noise temperature of the visible half of the sky T'_{sky} is 400 K at 144 MHz, and 40 K at 432 MHz. A value of 290 K is assumed for T_e. It is interesting to find that the values of T_{acs} obtained using the Tailor-equation virtually coincide with the values obtained from practical measurements.

Finally, the T_{acs}-values were calculated for various antenna beamwidths. The antennas used for 432 MHz have a narrower beamwidth than the areas of the cold sky region, which means that no dependence of the antenna temperature on the beamwidth results.

6. TEMPERATURE CALCULATION FOR AN ANTENNA POINTING TO A RADIO SOURCE

Based on the T_{sky}-data, it is possible using equation 3 to obtain T_{asky}, which is the temperature of an antenna that is pointed to the sky around a radio source but **without** the radio source itself. In order to obtain the total antenna temperature T_a **with** radio source, it is necessary to add T_{asky} and the temperature increase caused by the radio source.

The intensity of a radio source, that is its flux, is determined from the equivalent noise temperature T of the source, its spatial angle Ω_s, and the wavelength of the radiation:

$$S = (2kT\Omega_s)/\lambda_2 \text{ in W/m}^2\text{Hz} \qquad \text{(Eq. 5)}$$

The flux density-values (S) of certain radio sources were measured at various frequencies. Figure 1 is the result of these values.

The noise power that an antenna receives from a radio source is to be designated P_{as},

G(dB)	18	19	20	21	22	23	24	25	26
	CASSIOPEIA-A								
T_{as}(K)	87	109	138	173	218	275	346	435	550
T_{asky}	684	695	705	713	717	721	725	728	730
T_{sky}	725	738	750	760	765	770	775	778	780
T_a	771	804	843	886	935	996	1071	1163	1280
	CYGNUS-A								
T_{as}	84	106	134	169	211	268	336	423	536
T_{asky}	852	873	889	895	902	906	908	910	910
T_{sky}	930	955	975	982	990	995	998	1000	1000
T_a	936	979	1023	1064	1113	1174	1244	1333	1446
	SAGITTARIUS-A								
T_{as}	28	35	45	56	70	89	112	141	178
T_{asky}	2238	2296	2349	2381	2418	2443	2460	2476	2492
T_{sky}	2620	2690	2755	2795	2840	2870	2890	2910	2930
T_a	2266	2331	2394	2437	2488	2532	2572	2617	2670
	TAURUS-A								
T_{as}	12	15	18	23	29	37	47	59	74
T_{asky}	571	578	582	586	588	590	594	597	598
T_{sky}	587	597	600	605	607	610	615	618	620
T_a	583	593	600	609	617	627	641	656	672
	VIRGO-A								
T_{as}	9	12	15	19	23	30	37	47	59
T_{asky}	329	326	324	321	319	317	316	315	315
T_{sky}	292	288	285	282	279	277	276	275	275
T_a	338	338	339	340	342	347	353	362	374
	COLD SKY (LEO)								
T_{acs}	266	263	260	257	255	253	251	250	250
	COLD SKY (AQUARIUS)								
T_{acs}	331	328	325	322	320	318	316	315	315

Table 1: The temperatures of five radio sources and two "cold" points at 144 MHz

and is dependent on the flux density S of the source, as well as on the effective aperture of the antenna A. Furthermore, it is necessary for a factor 1/2 to be inserted, since most antennas only receive a certain polarization, whereas cosmic radio sources usually radiate unpolarized waves.

It is now possible for us to make a formula for T_{as}, which is the increase of the antenna temperature due to the reception of noise power from a radio source:

$$P_{as} = \frac{S \times A}{2} \quad \text{with}$$

$$A = \frac{G \times \lambda^2}{4\pi}$$

$$P_{as} = k \times T_{as}$$

$$T_{as} = \frac{P_{as}}{k} \quad \text{or}$$

$$T_{as} = \frac{S \times G \times \lambda^2}{8\,k\pi} \qquad \text{(Eq. 6)}$$

G(dB)	26	27	28	29	30	31	32	33
				CASSIOPEIA-A				
T_{as} (K)	26	33	41	52	65	82	103	130
T_{asky}	97	98	98	99	99	100	100	100
T_{sky}	66	67	67	68	68	69	69	70
T_a	123	131	139	151	164	182	203	230
				CYGNUS-A				
T_{as}	25	32	40	50	64	80	101	127
T_{asky}	104	104	104	104	104	105	105	105
T_{sky}	74	74	74	74	74	75	74	75
T_a	129	136	144	154	168	185	206	232
				SAGITTARIUS-A				
T_{as}	13	16	20	25	32	40	50	64
T_{asky}	232	233	235	237	238	239	240	241
T_{sky}	230	232	234	236	238	239	240	241
T_a	245	249	255	262	270	279	290	305
				TAURUS-A				
T_{as}	7	8	10	13	17	21	26	33
T_{asky}	70	71	72	73	73	74	75	76
T_{sky}	33	34	35	36	37	38	39	40
T_a	77	79	82	86	90	95	101	109
				VIRGO-A				
T_{as}	3	4	4	5	7	9	11	14
T_{asky}	60	60	60	60	60	60	60	60
T_{sky}	20	20	20	20	20	20	20	20
T_a	63	64	64	65	67	69	71	74
				COLD SKY				
				$T_{acs} = 60$				

Table 2: The temperatures of five radio sources and the cold sky at 432 MHz

Since the noise powers are added in the antenna, and after taking into consideration that the noise power divided by the Boltzman constant results in the equivalent noise temperature, a simple addition of T_{asky} and T_{as} will result in T_a. This is the temperature of an antenna pointing towards a cosmic radio source together with the "hot" sky around it, and including a pointing error (see section 4), as well as considering the effect of sidelobes facing towards the "warm" earth, and to the side. All these components were determined as a function of the beamwidth of the main lobe of the antenna. The results are given for each radio source separately in the tables. **Table 1** shows the temperature values for 144 MHz, and **Table 2** the same for 432 MHz.

The flux density values for all sources were obtained by arranging the measuring results given in the references. The values for Cassiopeia-A were obtained from the values from previous years calculated together with the known reduction rate for 1982. This reduction of the flux density of Cassiopeia-A is caused by the rapid expansion, and thus cooling of this residual part of a Super-Nova of approximately 400 years ago **(Table 3).**

Since the accuracy of the whole method is dependent on exact flux density values, these must be checked in several ways. For instance, the values for 144 MHz were obtained from measured values for 136 and 160 MHz by interpolation, however, this was not made in a linear manner, but after taking the spectral distribution of the radio source in question into consideration.

7. USING THE TABULAR VALUES

With the aid of the hot/cold method, it is possible to calculate the noise temperature of a receiver T_{rx} very exactly, if one uses the T_a of a certain radio source as hot, and T_{acs} as cold temperature. In order to do this, however, it is necessary to know the gain of the antenna.

$$T_{rx} = \frac{T_a - Y \times T_{acs}}{Y - 1} \qquad \text{(Eq. 4a)}$$

Firstly point the antenna to one of the cold regions of the sky, and then to one of the radio sources, after which the difference in the noise power between both antenna settings is measured. This is the factor Y for the above equation, and must not be inserted in dB. The same precautions (3) must be made when measuring Y, as with normal noise figure measurements.

The value for T_a is taken from Table 1, or Table 2 for the selected radio source, after taking the gain of the antenna used into consideration.

The receiver noise temperature T_{rx} in Kelvin can be converted easily into the usual noise figure after transposing equation 1:

$$F = 1 + \frac{T_{rx}}{290} \qquad \text{(Eq. 1a)}$$

and $$NF = 10 \log F$$

Radio source	Flux 10^{-22} (W/m^{2}Hz) 144 MHz	432 MHz	1296 MHz
CASSIOPEIA-A*	1.11	0.47	0.20
CYGNUS-A	1.08	0.46	0.17
SAGITTARIUS-A	0.36	0.23	0.14
TAURUS-A	0.15	0.12	0.095
VIRGO-A	0.12	0.05	0.02

* 1982

Table 3: Flux density values for five radio sources at 144, 432, and 1296 MHz

8. USING THE DIAGRAMS

In order to find T_{rx} with the aid of the tables, it is necessary to know the gain of the antenna used. It is possible, in the opposite manner, to calculate the antenna gain if T_{rx} is known – calculated from the measured noise figure NF, or the noise factor F.

In order to make this simpler for the user, and especially to allow the calculation with intermediate values of G and T_{rx}, diagrams have been drawn. They show T_{rx} as a function of Y for the four strongest radio sources, and for the cold sky using the antenna gain as parameter.

Since two cold points in the sky are available for 144 MHz, namely in the vicinity of constellation Leo and Aquarius, the diagram lines for this frequency are plotted twice.

Figure 4 shows the values of the strongest radio source, Cassiopeia-A, referred to the cold sky in Leo, as well as for Cygnus-A, referred to Taurus-A. (These lines fit into this diagram without interfering – see 8.1.)

Figure 5 shows the lines for Cassiopeia-A, referred to the cold sky in Aquarius, as well as Cassiopeia-A, referred to Taurus-A. The way to work with these diagrams is to be described later.

Figure 6 shows the lines for the other three strong radio sources, Cygnus-A, Sagittarius-A, and Taurus-A, referred to the cold sky in Leo, and, **Figure 7** finally shows the same three radio sources, referred to Aquarius.

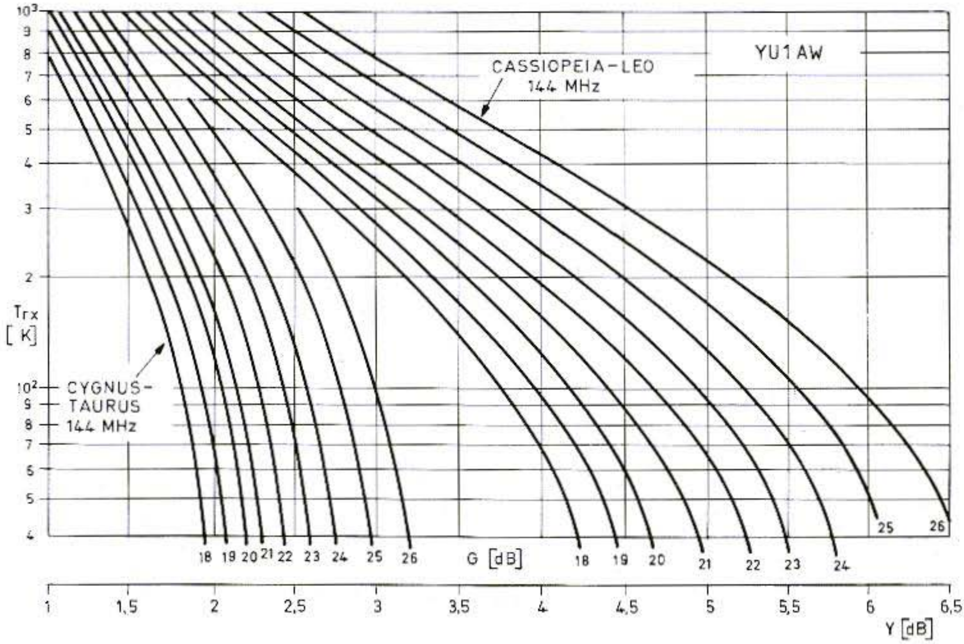

Fig. 4: Receiver noise temperature T_{rx} in Kelvin at 144 MHz using the Y-factor with the antenna gain as parameter. For Cassiopeia/Leo and Cygnus/Taurus

The most important thing is that one firstly uses the correct diagram, and secondly the correct scale. It could have been arranged more clearly if each group of parameters had its own diagram, but that would take too much space in the magazine.

In the case of 432 MHz, the diagram given in **Figures 8, 9, and 10** are valid. They contain the values for the same four radio sources, referred to a cold sky at 432 MHz.

One uses these seven diagrams firstly by simply inserting Y in dB (measured with the radio source in question as noise increase with respect to the appropriate cold sky). If T_{rx} is already known, it is possible for the antenna gain to be read off directly, and vice versa.

8.1. Ratio Measurement using Two Sources

If one compares the T_a-values of the various radio sources to another, one will see that they can be split into two groups: "hot" and "cold". Cassiopeia-A, Cygnus-A, and Sagittarius-A can be classed as "hot", whereas Virgo-A and Taurus-A are relatively "cold". Considering the importance of T_{cs} for the accuracy of the measurement, it is logical, not to point the antenna towards a cold region of the sky (Leo, Aquarius), but to one of the relatively cold radio sources. Figures 4 and 5 therefore contain two such pairs for 144 MHz.

8.2. Measuring Procedure

The most important thing is that no single

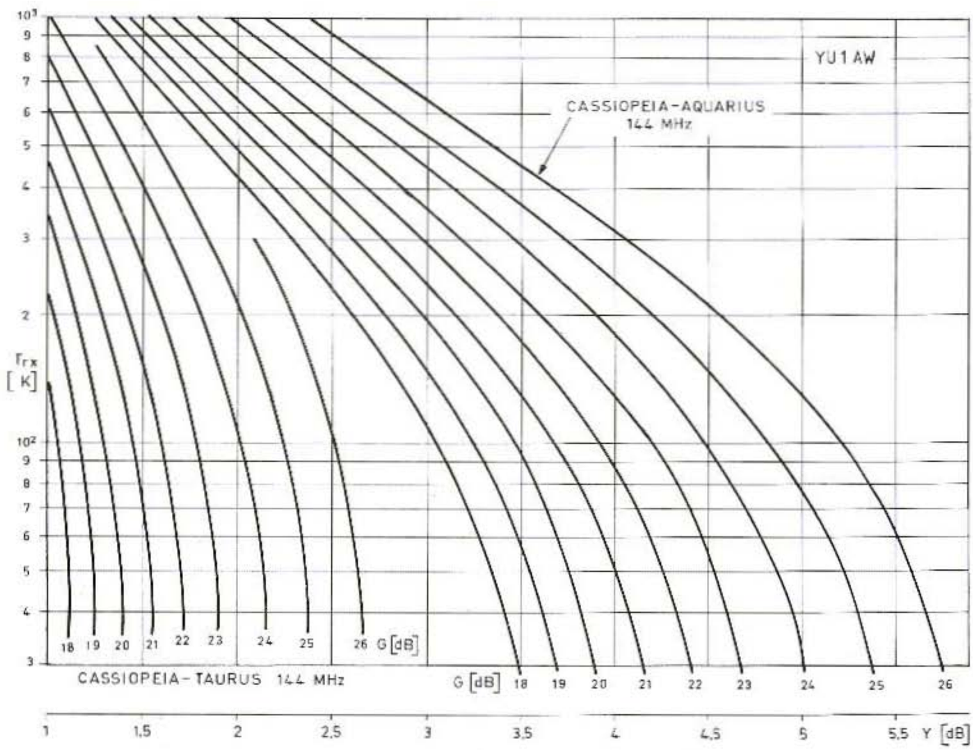

Fig. 5: as Fig. 4, but for Cassiopeia/Aquarius and Cassiopeia/Taurus

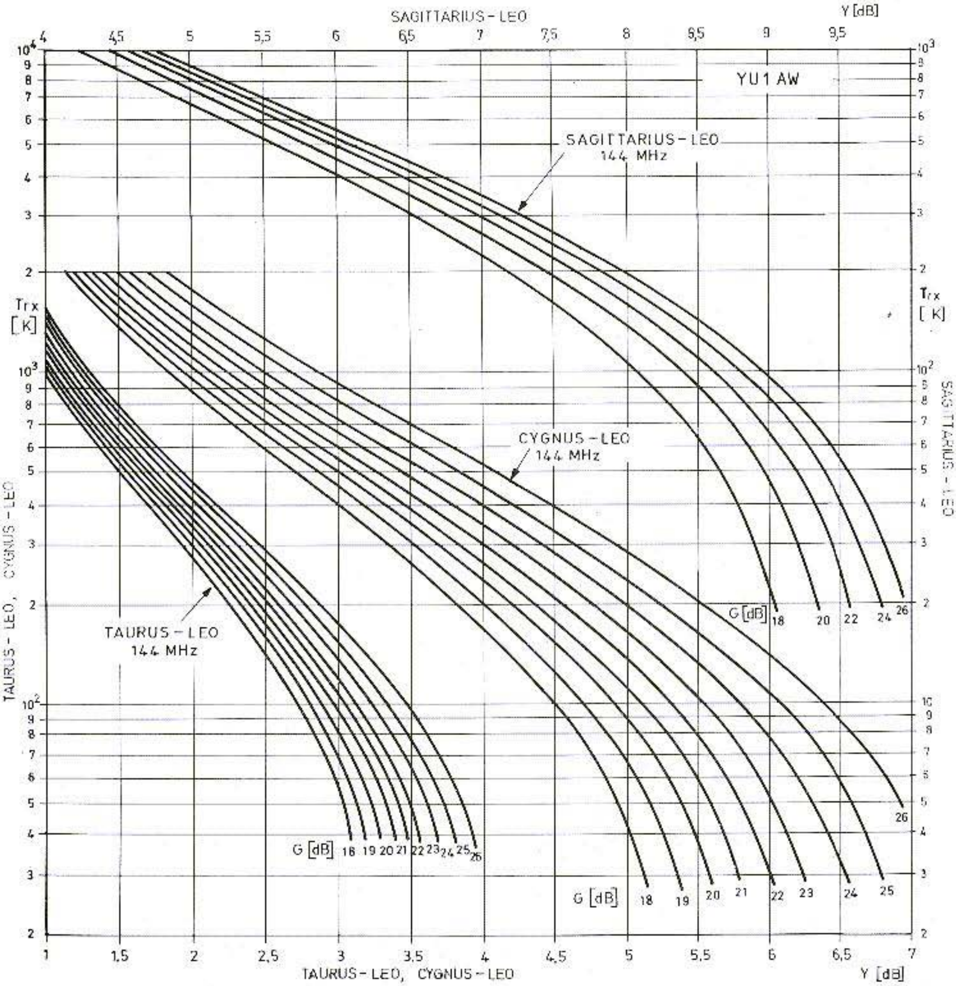

Fig. 6: as Fig. 4, but for Sagittarius/Leo and Taurus/Leo

stage of the complete receive system including all preamplifiers and converters is operating in a non-linear range. Once again, we would like to draw your attention to the article given in (3). The receiver is aligned to the widest bandwidth, SSB-mode, and the automatic gain control switched off. The noise voltage is now measured at IF-level, or, if not possible, at AF-level, according to the measuring equipment available. The accuracy of the measurements is dependent on the linearity and stability of the receive system, as well as on the precision of the calibrated attenuator and reading, and also on the accuracy of the antenna pointing system (rotators). The diagrams and calculations are very accurate, which means that any errors caused by them will only amount to a few Kelvin.

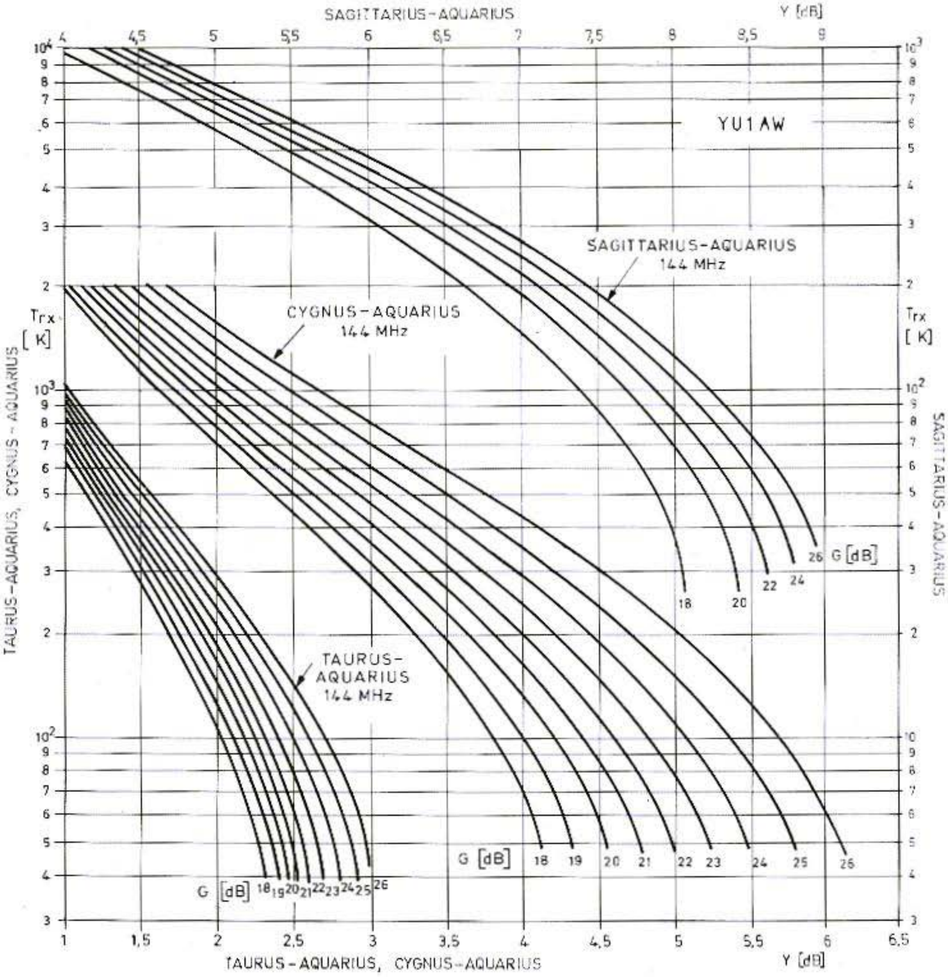

Fig. 7: as Fig. 4, but for Sagittarius/Aquarius, Cygnus/Aquarius, and Taurus/Aquarius

In order to average the statistical fluctuations of noise measurements, it is very necessary to carry out several measurements, preferably using various radio sources and "cold" points. Finally, one should form a mean value of all measurements.

9. FINAL NOTES

The given data allows exact measurements of the receive system parameters to be carried

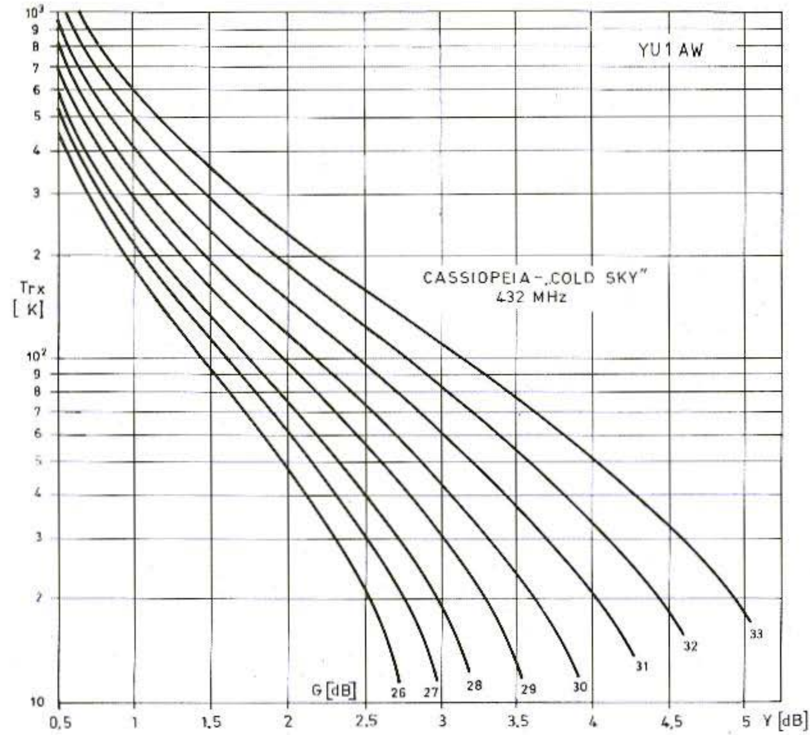

Fig. 8: Receiver noise temperature T_{rx} in Kelvin at 432 MHz using the Y-factor with the antenna gain as parameter for Cassiopeia/cold sky

out by using cosmic radio sources as references. The accuracy of this method is directly dependent on the accuracy with which one measures the ratio of noise powers between the hot and cold points in the sky.

During the preliminary phase, the assistance and literature published by Mr. Aleksander Tomik, Director of the Astronomic Observatory in Belgrad, was very helpful.

The practical application and checking of the method was made by Mr. Teodor Mrksic, YU7AR, and others. He made his array of four YU0B-antennas (4 × 22 el.) available for all measurements at 144 MHz. Also recently published measured values together with other EME-antennas were a great help in order to check the method.

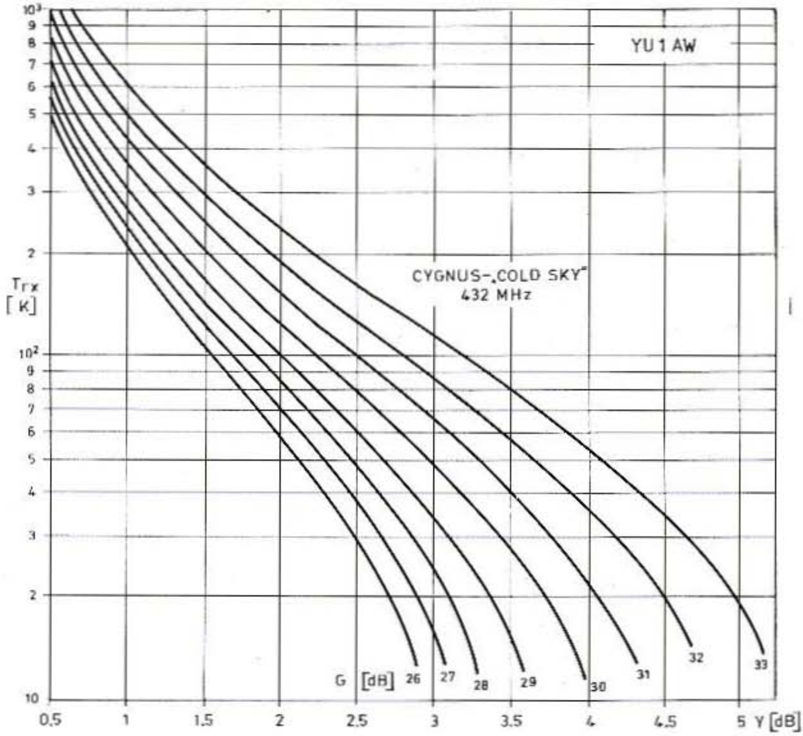

Fig. 9: as Fig. 8, but for Cygnus/cold sky

Only the strongest radio sources were considered in this article, since it is only possible for these to be used with relatively inexpensive equipment. In the references, it is possible for data to be obtained for the nebulars Omega and Aquila, which were measured by several owners of large EME-antennas, both at 144 MHz and at 432 MHz. These two nebulars generate, however, such a low flux density that (amateur) measured values for them are actually measurements of the sky around them. Since both are also in the vicinity of the center of the Milky Way, the noise temperature of the sky around them is relatively high, which means: $T_a = T_{asky}$.

Special care is always necessary when carrying out measurements in the sky in the vicinity of the center of the galaxy, due to the strong radiation from this area. This is especially so when using antennas with relatively low gain (large beamwidth).

In the frequency range in excess of 1 GHz, the flux density of most radio sources is very low **(Table 3)**, which means that the measurements described in this article will provide very inaccurate results inspite of the very low temperatures of the cold points in the sky. For

Radio source	Rectascension α	Declination δ
CASSIOPEIA-A	$23^h 21^m$	$+58° 32'$
CYGNUS-A	$19^h 57^m$	$+40° 36'$
SAGITTARIUS-A	$17^h 44^m$	$-29°$
TAURUS-A	$05^h 31^m$	$+22°$
VIRGO-A	$12^h 28^m$	$+12° 40'$

Table 4: Sky coordinates for the five radio sources used

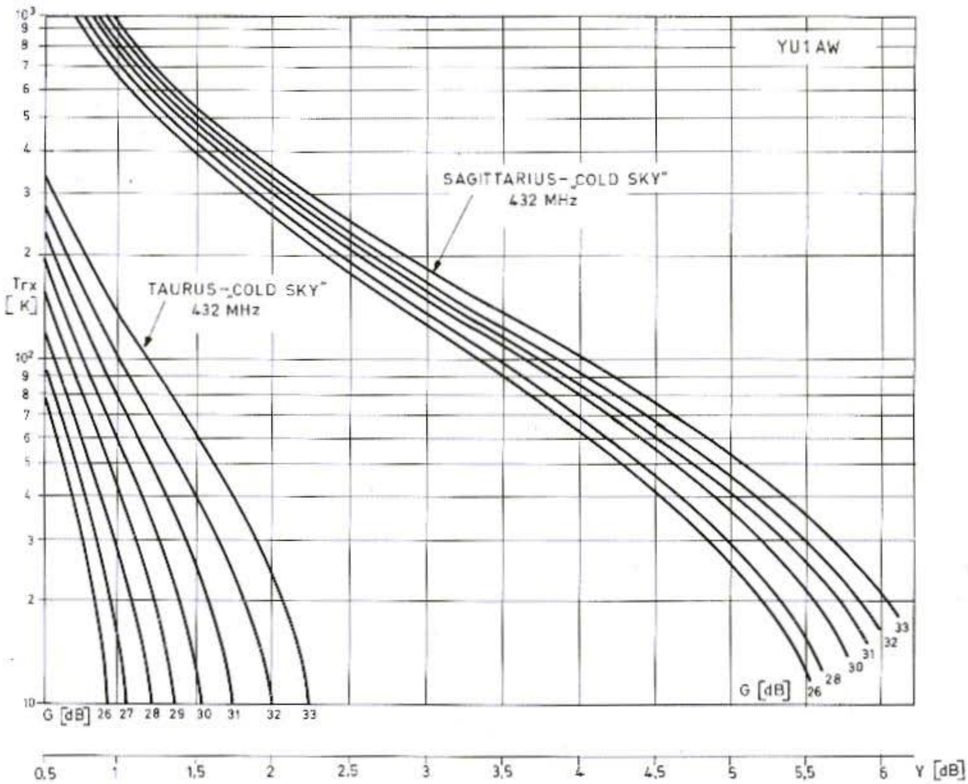

Fig. 10: as Fig. 8, but for Sagittarius/cold sky, and Taurus/cold sky

higher frequencies, it is therefore advisable to use the earth as source of the "hot" temperatures (290 K) and to measure it against the cold sky (T_{cs} = 10 K; T_{acs} = 30 K).

Attention should be paid when pointing the antenna to the earth surface that this does not deteriorate the matching, and that the antenna only "sees" the warm earth.

Cold sky Constellation	Rectascension α	Declination δ	Temperature T_{cs} 144 MHz	432 MHz
Leo	$09^h 30^m$	+40°	195 K	15 K
Aquarius	$22^h 30^m$	0°	275 K	20 K

Table 5: Sky coordinates for the two "cold" points

Tables 4 and 5 finally give the sky coordinates for the radio sources and cold points used.

10. REFERENCES

(1) G. Hoch, DL6WU:
Determining the Sensitivity of Receive Systems with the Aid of Solar Noise
VHF COMMUNICATIONS 12,
Edition 2/1980, pages 66-72

(2) R. F. Taylor/F. J. Stocklin:
VHF/UHF stellar calibration error analysis 1971

(3) J. Gannaway, G3YGF/
D. Holmes, G4FZZ
Some Pitfalls in Noise Figure Measurements
VHF COMMUNICATIONS 13,
Edition 1/1982, pages 44-48

(4) Radio Sky Maps
Proc. of the IEEE, April 1973

(5) J. D. Kraus
Radio Astronomy McGraw-Hill, New York

(6) Radio Noise and Interference
Kap. 27 in:
Reference Data for Radio Engineers
ITT/Howard W. Sams + Co. Inc.

Konrad Hupfer, DJ 1 EE

A 10 W Linear Amplifier for the 23 cm Band

Although SHF power amplifiers for the 23 cm band are available on the market, we hope that the circuit described in this article will be attractive to those readers wishing to construct their own equipment for this frequency range. The 10 W power output from this single-stage amplifier allows communications to be made over considerable distances. Of course, one can also use it to drive a high-power amplifier equipped with tubes that is mounted at the antenna, or at least just under the roof. This is a great advantage for operation over the L-transponder of OSCAR 10!

The transistor used in this amplifier has been on the market for several years now, and several experiments have been made with it. However, at that time it seemed too expensive for publication of an amateur linear amplifier. Although this transistor can still not be classed as inexpensive, the author considers that one cannot continue to wait until this transistor only costs a few DM. Finally, the ready-made linear amplifiers available on the market for this frequency range are also not inexpensive.

In order to keep the PC-board as inexpensive as possible, the circuit is built up in a semi-printed construction, that is only the UHF-lines use PTFE-glass fibre material. The tuning elements are also less expensive types, although an improvement of gain and efficiency could be achieved with air-spaced microwave trimmers (Johnson, Tekelec, etc.) as well as simpler alignment.

1. CIRCUIT DETAILS

As can be seen in the circuit diagram given in **Figure 1**, the transformation networks at input and output possess two trimmers each, in order to compensate for all possible tolerances of the transistors, and installation – emitter soldering, base and collector connections. This means that this construction can also be used for experimentation; the "UHF-wiring" is not critical, and no accuracies of a tenth of a millimeter are required.

As has often been discussed in conjunction with UHF power amplifiers, a through ground connection is necessary from the "base-ground side" via the emitter support to the "collector-ground side". This is made with the aid of a thin copper foil (approx. 0.1 mm).

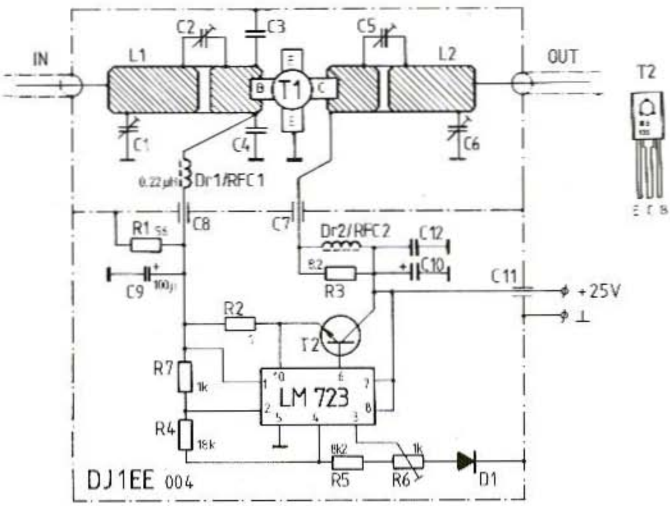

Fig. 1: Single-stage 10 W linear amplifier for 1296 MHz

The collector voltage supply is made via an approximately 15 mm long piece of 0.8 mm dia. enamelled copper wire.

Special attention has been paid to the generation of the quiescent current and its stabilization (1). An integrated voltage stabilizer LM 723 generates a variable base-bias voltage (R 6) with an impedance of approximately 50 mΩ together with a power transistor (T 2). An increase in temperature of the emitter support of T 1 (UHF-transistor) heats diode (D 1), which is mounted on this support; this diode controls the voltage stabilizer so that the base-bias voltage is controlled back.

Since this linear amplifier is designed as power amplifier for connection to conventional transverters having an output power of between 1 and 3 W, the UHF-connections are made in the form of coaxial cable (preferably this PTFE-cable) and are directly soldered to the input and output of the transformation networks. They can then be provided with the correct length for the application in question.

2. COMPONENTS

T 1:	BLW 98 (Philips) or TH 598 (Thomson-CSF)
T 2:	BD 135 or similar NPN silicon transistor (45 V/1.5 A)
I 1:	LM 723 integrated voltage stabilizer
D 1:	1N4001 or similar 1A-Diode
C 1, C 6:	Plastic foil trimmer 6 pF, Philips: grey
C 2, C 5:	Plastic foil trimmer 5 pF, Seiko: green
C 3, C 4:	Ceramic disk capacitor, 0.5 pF
C7, C8, C 11:	Feedthrough capacitors of approx. 100 pF for solder mounting
C 9:	Alu. electrolytic 100 µF/6 V
C 10:	Tantalum electrolytic approx. 4.7 µF/30 V
C 12:	Ceramic disk capacitor approx. 1 nF

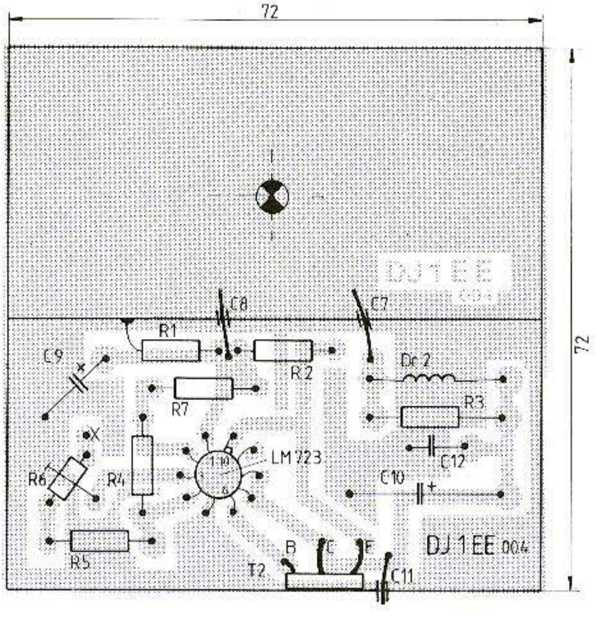

Fig. 2:
The epoxy PC-board DJ1EE 004 is equipped from the copper side

RFC 1:	Miniature ferrite choke 0.22 μH (Delevan)
RFC 2:	6-hole ferrite core choke (Philips)
L 1, L 2:	Strips of double-coated PTFE-PC-board material, 1.4 mm thick, soldered as shown in **Figure 3** to the ground surface of PC-board DJ1EE 004
R 1:	56 Ω
R 2:	1 Ω
R 3:	8.2 Ω
R 4:	18 kΩ
R 5:	8.2 kΩ
R 6:	1 kΩ trimmer potentiometer
R 7:	1 kΩ

3. CONSTRUCTION

The amplifier is accommodated on the copper side of a single-coated epoxy PC-board, whose dimensions are 72 mm x 72 mm. This board, which has been designated DJ1EE 004, is shown in **Figure 2.** It can be accommodated in a conventional metal box of 74 x 74 mm. The PC-board and case should be mounted on a sufficiently large heat sink with the aid of several screws and the transistor bolt.

The PC-board is not etched in the area of the UHF-amplifier. A hole is drilled in the center of this part of the board into which transistor T 1 is mounted so that its emitter connections are flat on the ground surface. **Figure 3** shows the positions of striplines L 1 and L 2, as well as the trimmers, fixed capacitors, and chokes at the base and collector. The intermediate panel in the center of the case screens the UHF-portion from the DC-circuit, and this is not shown in Figure 3.

Installation details for the UHF-transistor and the diode used for temperature compensation are shown in **Figure 4.** The prototype does not look very professional **(Figure 5),** since the board was cut by hand. Due to the reflections on the surface of the solder, it is difficult to see the striplines, trimmers, and capaci-

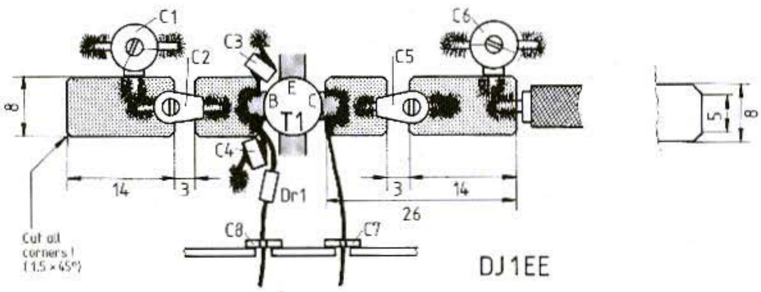

Fig. 3: Dimensions and construction of the stripline circuits comprising double-coated PTFE PC-board material

tors. The holes in the heat sink have nothing to do with this article; it was left over from a previous project.

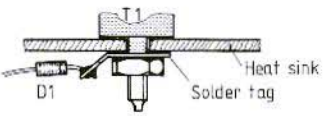

Fig. 4: UHF-power transistor and mounting of the diode for temperature compensation of the quiescent current

4. CONNECTION AND ALIGNMENT

After checking the linear amplifier for incorrect wiring and component faults, all trimmers should be set to a central position. It is advisable to firstly check the U_{BE} control circuit on its own, and to connect a conventional 1 A-diode instead of the base of the UHF-transistor.

A voltage between 0.4 and 0.8 V should now be selected with the aid of potentiometer R 6. If this is the case, align the potentiometer to exactly 0.5 V and remove the operating voltage. The base of T 1 is now connected.

For carrying out the next step, the output of the amplifier must be terminated with a suitable 50 Ω load – preferably a power meter or reflectometer.

The circuit is now provided with an operating voltage of 25 V, and a collector-quiescent current of 250-300 mA is adjusted with the aid of R 6. The final UHF-alignment is made according to **Figure 6** by slowly increasing the UHF-drive as measured using a calibrated reflectometer.

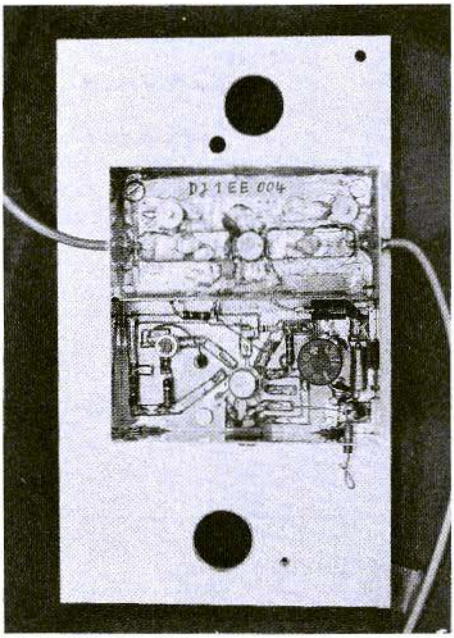

Fig. 5: Prototype of the linear amplifier in a metal box mounted on an old heat sink

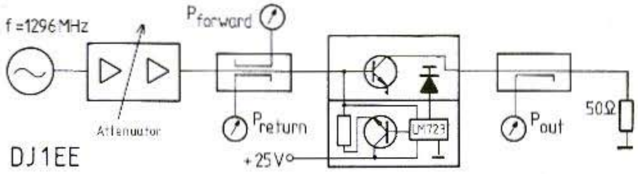

Fig. 6:
Measuring circuit alignment

The matching networks are aligned alternately for maximum output power (C 5, C 6) and best matching at the input (C 1, C 2). The output power should amount to 10 W at a drive power of 3 W. The collector current should increase from its quiescent value to approximately 0.9 – 1 A.

Finally, the author would like to mention experiments that he has recently made with a new NEC-transistor, type NEL 1320 81-12: When using a similar circuit to that described, the following preliminary values were measured:

Operating voltage:	**13,5 V**
Quiescent current:	170 mA
Drive power:	4 W
Output power:	17 W
Efficiency:	approx. 45%

If there is sufficient interest, a linear amplifier using this transistor could be described later.

5. REFERENCES

(1) MOTOROLA
RF-Data Manual, 1980

Knut Brenndörfer, DF8CA

A 5/50 W Power Meter with Dummy Load for Operation up to 1.3 GHz

Many different types of power meters are used by radio amateurs. Most of the power meters available on the market do not cover up to this frequency range, and their accuracy is much less than required by VHF-UHF radio amateurs. In addition to this, many through-line wattmeters show a dependence of the reading on the impedance of the antenna. This problem is solved when using power meters equipped with a built-in terminating resistor (dummy load).

This terminating resistor was the component that caused problems in the past, however, nowadays one can purchase industrial products having excellent specifications, and even amateur prices.

1. PRINCIPLE OF OPERATION

The various methods of RF-power measurements were already discussed in (1). For this reason, we are only to discuss such power measurements in conjunction with a terminating resistor.

Figure 1 shows the basic circuit used. It will be seen that the circuit does not allow a true power measurement, but measures the voltage, which can be recalibrated into power, since the resistance remains constant.

The required calibration causes great difficulties to most home constructors. The described circuit uses halfwave rectifiers using a diode. The consideration was: why couldn't this diode be used to rectify a frequency of 100 MHz in the same manner as a voltage having a frequency of 50 Hz?

If rectifier diodes type 5082-2800, manufactured by HP, are used, one will see from the specifications of the diode that this assumption is true. Of course, the switching times and circuit capacitances do have their effect, but an experimental circuit showed that usable results were provided up to 1.3 GHz, since the capacitive shunt was within limits due to the

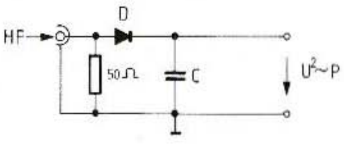

Fig. 1: RF-power measurement made by measuring the voltage across a 50 Ω terminating resistor

use of three diodes. Since voltages with a frequency of 50 Hz are usually available, and can be measured exactly, these can be used for calibrating the wattmeter.

2. SELECTION OF THE COMPONENTS

The heart of the circuit is the terminating resistor manufactured by CTC (ACRIAN). It comprises a resistor layer, which has been oxydized onto a beryllium-oxide plate. This is provided with a flange that allows it to be mounted on the heat sink. The most interesting models for radio amateurs are the following:

TA 150-50 with a rating of 150 W and an upper frequency limit of 2 GHz, and
TC 250-50 with a rating of 250 W and a frequency range of up to 1 GHz.

Type TA 150-50 was selected for the author's prototype. The excellent return-loss specifications are given in **Figure 2.**

Before selecting the rectifier diode, one should know that it must be able to handle the peak-to-peak voltage present across the 50 Ω resistor. This voltage is calculated according to the following equation:

$U_{ppD} = 20 \times \sqrt{P}$
where: P in W into 50 Ω

In the case of a power of 50 W, this amounts to 141.42 V, which would be rather too much for a diode having a maximum junction voltage of 70 V.

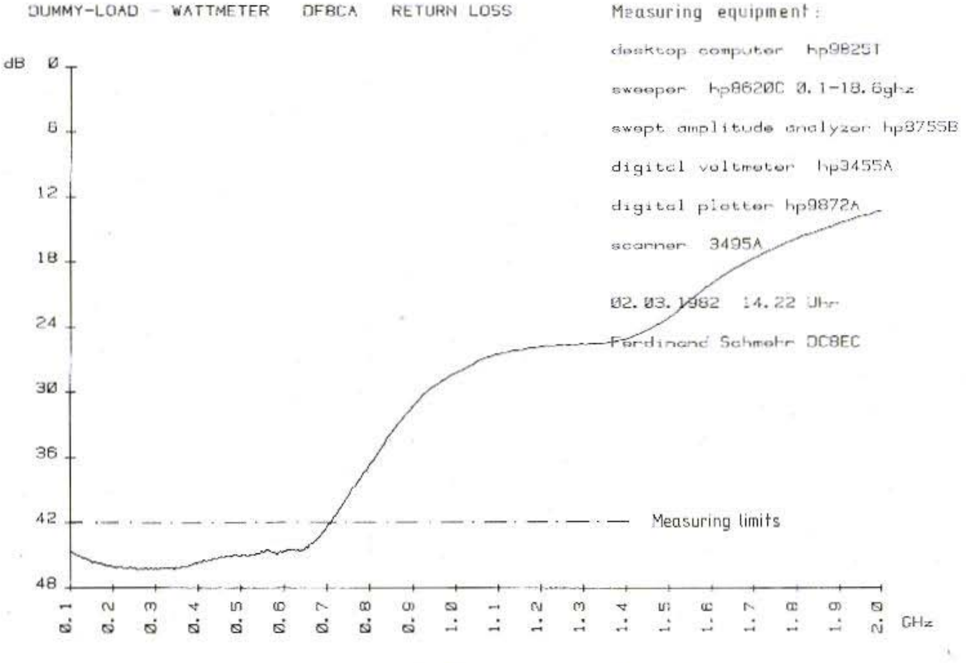

Fig. 2: Return loss of the complete wattmeter in the range of 100 MHz to 2 GHz

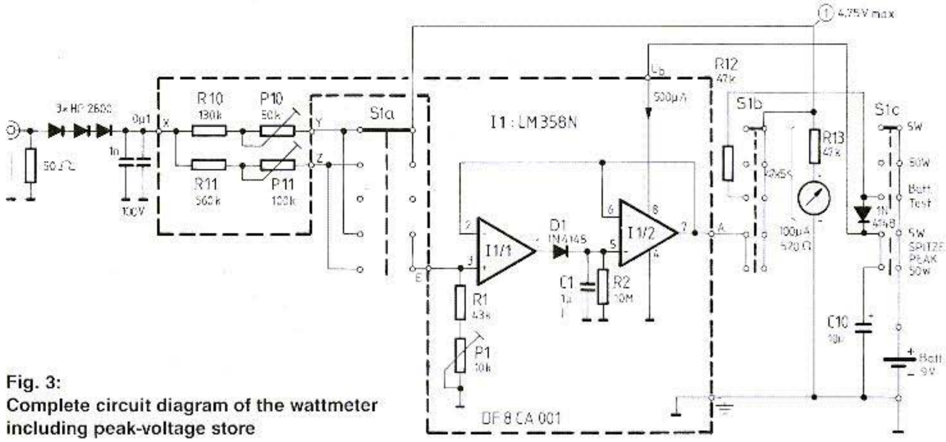

Fig. 3: Complete circuit diagram of the wattmeter including peak-voltage store

In order to have some reserve, three diodes are connected in series. Some reserve should also be allowed for the terminating resistor since these small ceramic plates are very sensitive to overload due to their low heat capacity, even if it is only for a fraction of a second.

3. OVERALL CIRCUIT

Figure 3 shows the complete circuit diagram of the wattmeter. One will see the terminating resistor, rectifier diodes, and charge capacitor, which is formed by the parallel connection of a 1 nF chip capacitor and a 0.1 µF ceramic capacitor. The dropper resistor of the 100 µA-meter is split into two so that a maximum of 4.75 V can appear at point (1).

The rest of the peak voltage present across the charge capacitor is dissipated in R 10, P 10, or R 11, P 11. Resistor R 13 is designed so that 4.75 V at point (1) result exactly at full scale. The voltage across the charge capacitor results from the peak voltage across the 50 Ω resistor, that is:

$U_p = \sqrt{2} \times \sqrt{P \times R}$.

In order to be able to measure the power peaks of SSB-signals more accurately, the instrument was equipped with a peak-voltage storage. The circuit is constructed according to (2) and has a gain of exactly one.

Resistors R 1 and P 1 form the impedance of the meter including dropper resistor R 13, since the operational amplifier is high-impedance at the input. The double op. amp. used is a LM 358 N and operates down to the negative operating voltage, which means that no plus/minus supply is required.

The parts of the circuit enclosed within the dashed lines are accommodated on a PC-board, which has been designated DF8CA 001. The component locations on the 70 mm x 33 mm single-coated PC-board are as shown in **Figure 4.** A photograph of the completed board is given in **Figure 5.**

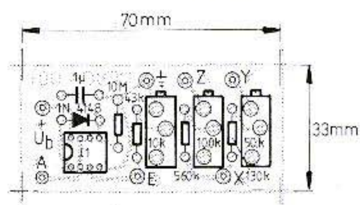

Fig. 4: Components of the single-coated PC-board DF8CA 001 for accommodation of the peak-voltage storage and two dropper resistors

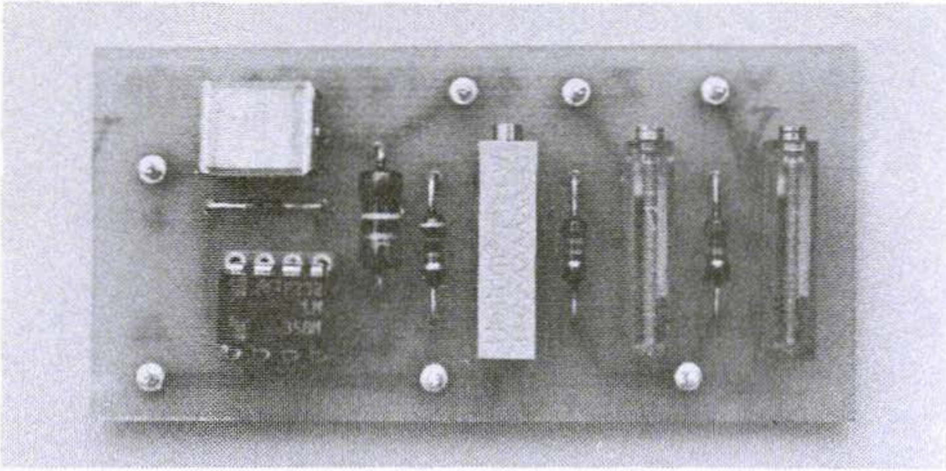

Fig. 5: Photograph of the completed board

4. CONSTUCTION

It is necessary for the 50 Ω terminating resistor to be mounted on a sufficiently large heat sink. Attention should be paid that the surface is smooth and that the heat-contact is as good as possible.

In the case of the author's prototype, the RF-input is made with the aid of a piece of PTFE-coaxial cable RG-142 B/U (similar diameter to RG-58), which leads to an N-flange connector with cable connection. Attention must be paid that no mechanical load is placed on the resistor. This is avoided by soldering the cable to a brass plate that is screwed to the heat sink.

The three diodes are soldered to the chip bypass capacitor using the shortest leads possible. The more compact the construction, the higher will be the upper cutoff frequency. **Figure 6** shows a photograph of the terminating resistor with the three diodes and charge capacitors. The mounting of the N-connector is shown in **Figure 7.**

The case was made by bending aluminium plate in the form of a U. However, another avail-

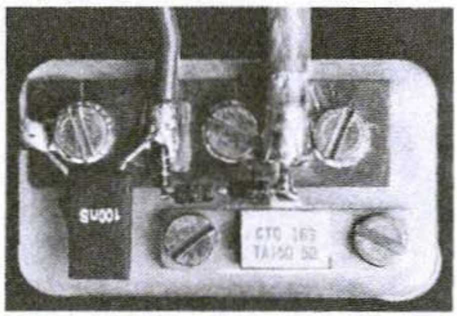

Fig. 6: Terminating resistor, diodes, and charge capacitor. It is not absolutely necessary to mill the mounting surface.

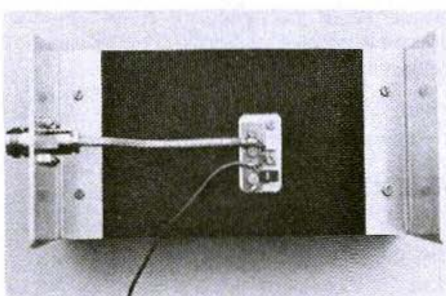

Fig. 7: Heat sink and lower part of the case

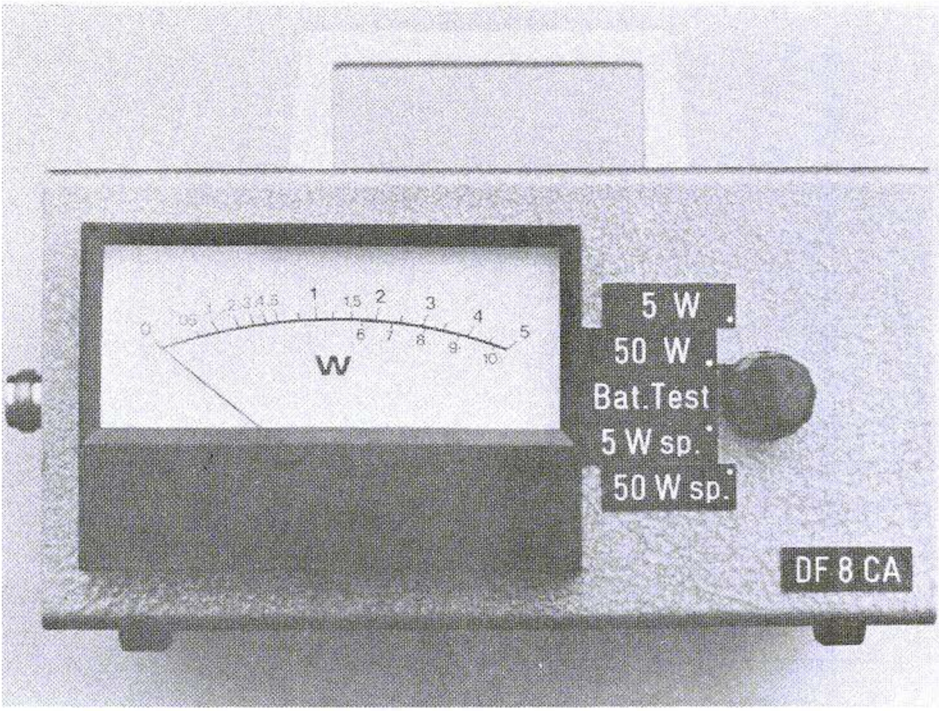

Fig. 8: Photograph of the completed wattmeter

able case can be used. The battery, the PC-board, and the four-way, six-pole changeover switch are mounted in the cabinet. The single contact from the charge capacitor to point X should be in the form of a plug-in contact. **Figure 8** shows a photograph of the completed wattmeter.

5. ALIGNMENT

The following are required for alignment:
A variable isolating transformer, and an accurate AC-voltmeter (digital voltmeter). In addition to this, a normal transformer of 220 V to 24 V/1 A is useful for low voltages, which can be connected to the output of the variable isolating transformer. Since the charge capacitor between point X and ground provides too low a value for a frequency of 50 Hz, one should provide an electrolytic of 50 to 100 μF in parallel with it temporarily during the alignment period!

Firstly, align for a RMS-voltage of:

$U_{RMS} = 7.07107 \times \sqrt{P}$
where P in W into 50 Ω

Thus: $U_{RMS} = 15.81$ V. The voltmeter should be aligned with P 10 in the 5 W-range for maximum reading (full scale).

The same is made at 50 V in the 50 W-range.

Power	RMS-voltage
50 W	50.00 V
45 W	47.43 V
40 W	44.72 V
35 W	41.83 V
30 W	38.73 V
25 W	35.36 V
20 W	31.62 V
15 W	27.39 V
12.5 W	25.00 V
10 W	22.36 V
7.5 W	19.37 V
5 W	15.81 V
4.5 W	15.00 V
4 W	14.14 V
3.5 W	13.23 V
3 W	12.25 V
2.5 W	11.18 V
2 W	10.00 V
1.5 W	8.660 V
1.25 W	7.906 V
1 W	7.071 V
0.75 W	6.124 V
0.5 W	5.000 V
0.4 W	4.472 V
0.3 W	3.873 V
0.2 W	3.162 V
0.1 W	2.236 V
0.05 W	1.581 V

Voltage values for calibrating the power scale

It is now possible for the intermediate values given in **Table 1** to be adjusted and marked on the scale with the aid of a pencil.

The alignment can, if necessary, also be carried out with DC-voltage. The values to be adjusted are, however, factor $\sqrt{2}$ greater than those given in Table 1. Attention should be paid, however, that the power at the 50 Ω resistor is **twice** as large during the alignment process than in normal operation. Due to the danger of overload, this method is not recommended.

Since the threshold voltage of the diodes has a different effect in both ranges, one should use two scales. However, the differences at 5 and 50 W are so small that one can use a scale having the mean value. If more sensitivity is required, in other words, several lower power ranges, it will be necessary to use different scales for each range.

However, a variation of the diode threshold voltage as a function of temperature can have such a strong effect in some cases that the measurement will be too inaccurate. At low power levels, the diode should be used in the square portion of its characteristic curve.

The alignment of the peak voltage storage is made by connecting a signal equal to full scale and aligning P 1 so that no difference results on switching from normal to peak-value indication.

For the battery test, R 12 is selected so that a voltage of 9 V should be in the last third of the reading.

The maximum errors of the described wattmeter are normally less than 10%.

A considerably higher accuracy can be achieved if a careful construction and alignment is made.

6. REFERENCES

1) Otto Frosinn, DF7QF:
A Home-Made UHF/SHF Power Meter
VHF COMMUNICATIONS 13,
Edition 4/1981, pages 221-229

2) Zirpel: Operationsverstärker
Franzis-Verlag München
ISBN3-7723-6132-3

MATERIAL PRICE LIST OF EQUIPMENT

described in edition 1/1984 of VHF COMMUNICATIONS

DB 1 NV	**10 GHz Transceiver with dielectric stabilized oscillator**		Art. No.	**Ed.4/83+1/84**
Doppler module FO-DP 12 KF as described in Edition 4/83			6833	DM 260.–
Flange micrometer		miniature, spindle dia. 3.5 mm	6832	DM 98.–
Components	DB 1 NV 001	8 transistors, 6 diodes, 3 ICs, 1 voltage regulator, 8 coil kits, 3 kinds of wires, 2 mini RF chokes, 2 foil trimmers, 7 foil, 14 ceramic caps. with 2.5 or 5 mm spacing, 6 ceramic or foil caps. with 7.5 mm spacing, 9 tantalum and 3 aluminium electrolytics, 11 ceram. bypass caps., 40 resistors, and PC-board double-coated, silver-plated, drilled	6831	DM 182.–
Kit	**DB 1 NV 001**	**with above parts**	**6837**	**DM 530.–**

DF 9 RL	**2400 Hz Generator for Sync. of the METEOR Satellites**			**Ed. 1/1984**
PC-board	DF 9 RL 002	single-coated, without plan, drilled	6834	DM 7.–
Components	DF 9 RL 002	1 crystal 3686.40 kHz, HC-43/U, 2 CMOS ICs, 2 diodes, 1 foil trimmer, 3 ceram. caps., 3 resistors	6835	DM 49.–
Kit	**DF 9 RL 002**	**complete with above parts**	**6836**	**DM 54.–**

UKW berichte Terry D. Bittan · Jahnstr. 14 · Postfach 80 · D-8523 Baiersdorf
Tel. West Germany 9133-855. For Representatives see cover page 2

Space and Astronomical Slides

Informative and Impressive

VHF COMMUNICATIONS now offers sets of phantastic slides made during the Gemini,Apollo,Mariner, and Voyager missions, as well as slides from leading observatories. These are standard size 5 cm x 5 cm slides which are framed and annotated.

Prices plus DM 3.00 for post and packing.

Sets of 5 NASA-slides DM 8.50 per set

Set 8103	Apollo 11: Earth and Moon
Set 8104	Apollo 11: Man of the Moon
Set 8105	Apollo 9 and 10: Moon Rehearsal
Set 8106	From California to Cap Canaveral
Set 8107	Apollo 12: Moon Revisited
Set 8108	Gemini Earth Views
Set 8109	Apollo 15: Roving Hadley Rille
Set 8110	Apollo 16: Into the Highlands
Set 8111	Apollo 17: Last voyage to the moon
Set 8112	Apollo 17: Last Moon Walks
Set 8113	Mariner 10: Mercury and Venus

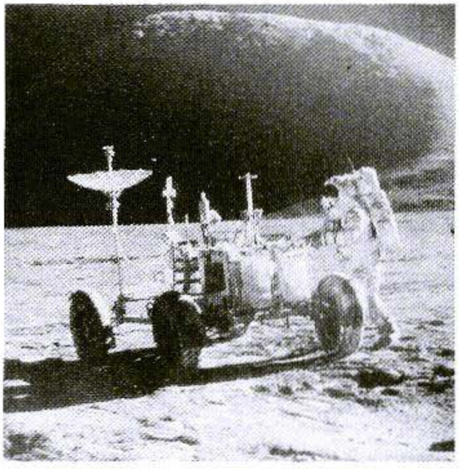

Set 8147 »Jupiter encountered« 20 slides of VOYAGER 1 & 2 DM 35.00

1. Jupiter and 3 satellites 2. The giant planet 3. Jupiter, lo and Europa 4. The Red spot 5. The Red spot in detail 6. The swirling clouds 7. lo and a white oval 8. The neighbourhood of the Red spot 9. The rings of Jupiter 10. The Gallilean satellites 11. Amalthea 12. Callisto 13. Impact feature on Callisto 14. Eruption on lo 15. lo full disc 16. Europa close-up 17. Europa distant view 18. Ganymede close-up 19. A distant Ganymede 20. The lovian system

Set 8100 »Saturn encountered«, 20 VOYAGER-1 slides DM 35.00

1. Saturn and 6 of its moons 2. Saturn from 11 mio miles 3. Saturn from 8 mio miles 4. Saturn from 1 mio miles 5. Saturn and rings from 900.000 miles 6. Saturn's Red spot 7. Cloud belts in detail 8. Dions against Saturn 9. Dione close-up 10. Rhea 11. Craters of Rhea 12. Titan 13. Titan's polar hood 14. Huge crater on Mimas 15. Other side of Mimas 16. Approaching the rings 17. Under the rings 18. Below the rings 19. »Braided« F ring 20. lapetus

Set 8148 »VOYAGER 2 at Saturn«, 20 VOYAGER-2 slides DM 35.00

1. VOYAGER 2 approaches 2. Clouds & rings 3. Storms & satellites 4. Cyclones, spots & jet streams 5. Convective regions 6. Atmospheric disturbance 7. Rings & shadows 8. The »C« ring 9. Ring details 10. The »A« ring 11. Looking back on Saturn 12. Titan – night side 13. Titan – atmospheric bands 14. The »F« ring 15. Hyperion close-up 16. lapetus revealed 17. Enceladus explored 18. The Tethys canyon 19. The »F« ring structure 20. Within the Enke division

Set 8101 »From Here to the Galaxies«, 20 astronomical slides DM 35.00

1. Moon – eastern limb 2. Moon – NE limb 3. Comet IKEYA SEKI 4. Trapezium 5. »Sunflower« planetary nebula in Aquarius 6. Nebula in Cassiopeia 7. North America nebula 8. Sagittarius star cloud 9. Spiral galaxy in Triangulum 10. Sp. gal. in Canes venatici 11. Sp. gal. in Coma Berenices 12. Sp. gal. in Leo 13. Edge-on sp. gal. in Virgo 14. Sp. gal. in Canes Venatici 15. Sp. gal. in Camelopardalis 16. Sp. gal. in Lynx 17. Sp. gal. in Pegasus 18. U.S. Naval Observatory Flagstaff, Ar. 19. 6-inch transit telescope 20. 61-inch reflector

Set 8102 »The Solar System«, 20 NASA/JPL slides DM 35.00

1. Solar System 2. Formation of the Planets 3. The Sun 4. Mercury 5. Crescent Venus 6. Clouds of Venus 7. Earth 8. Full Moon 9. Mars 10. Mars: Olympus Mons 11. Mars: Grand Canyon 12. Mars: Sinuous Channel 13. Phobos 14. Jupiter with Moons 15. Jupiter Red Spot 16. Saturn 17. Saturn Rings 18. Uranus and Neptune 19. Pluto 20. Comet Ikeya-Seki.

Set 8149 »The Sun in action«, 20 NASA/JPL slides DM 35.00

1. Sun in Hα light 2. Total Solar eclipse 3. Outer corona 4. Corona from SMM satellite 5. Corona close-up 6. Solar magnetogram 7. Active regions in X-radiation 8. X-ray corona 9. A coronal hole 10. Solar flare 11. Active Sun 12. Eruptive prominence 13. Gargantuan prominence 14. Eruptive prominence 15. Huge Solar explosion 16. Prominence in action 17. Sun in action 18. Magnetic field loops 19. Prominence close-up 20. Chromospheric spray

Set 8144 »Space shuttle«, 12 first-flight slides DM 24.00

1. STS1 heads aloft 2. View from the tower 3. Tower clear 4. Launch profile 5. Payload bay open 6. STS control Houston 7. In orbit, earth seen through the windows 8. Bob Crippen in mid-deck 9. John Young 10. Approaching touchdown 11. After 54.5 hours in space Columbia returns to Earth. 12. Astronauts Crippen and Young emerge after the successful mission

UKWberichte Terry D. Bittan · Jahnstr. 14 · Postfach 80 · D-8523 Baiersdorf
Tel. West Germany 9133-855. For Representatives see cover page 2

FOR OSCAR 10 AND NORMAL COMMUNICATIONS

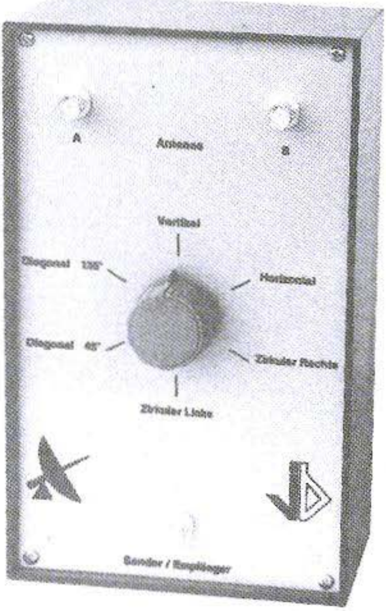

Polarisations Switching Unit for 2 m Crossed Yagis

Ready-to-operate as described in VHF COMMUNICATIONS. Complete in cabinet with three BNC connectors. Especially designed for use with crossed yagis mounted as an "X", and fed with equal-length feeders. Following six polarisations can be selected: Vertical, horizontal, clockwise circular, anticlockwise circular, slant 45° and slant 135°.

VSWR:	max. 1.2
Power:	100 W carrier
Insertion loss:	0.1 to 0.3 dB
Phase error:	approx. 1°
Dimensions:	216 x 132 x 80 mm

Low-Noise GaAs-FET Masthead Amplifiers for 144 MHz and 432 MHz MV 144 and MV 432

Selective High-Power Masthead Amplifiers in Waterproof cast-aluminium case with mast brackets. Built-in relay for transmit-receive switching. PTT via coaxial cable using supplied RF/DC-splitter.

- Noise figures: MV 144: 0.9 dB/0.6 dB
  (typ. values) MV 432: 1.0 dB/0.8 dB
- Overall gain: MV 144: 15/20 dB, switchable
  MV432 : 15 dB
- Insertion loss, transmit: typ. 0.3 dB
- Maximum transmit power:
  MV 144: 800 W SSB, 400 CW/FM
  MV 432: 500 W SSB, 250 CW/FM
- Operating voltage: 12 V via coaxial cable

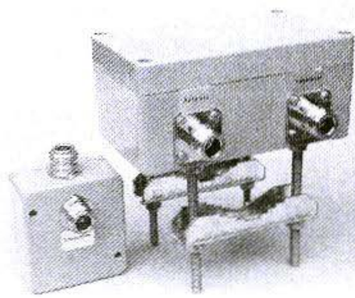

- Connections:
  N-Connectors
- Dimensions:
  125 x 80 x 28 mm
  (without brackets)

Further details on request.

UKW technik Terry D. Bittan · Jahnstr. 14 · Postfach 80 · D-8523 Baiersdorf
Tel.: West Germany 9133 / 855 · For representatives see cover page 2